REVIEW

Check for updates

Liquid crystal elastomers for solar, mechanical, thermal, and electrochemical energy applications

Meng Zhang,†[a] Xinxin Lu,†[b] Tingting Ye,†[b] Haodong Hu,†[c] James P. Scarbrough,[a] Rui Wang,[a] Yuxing Yao, [ID] *[b] Shucong Li*[c] and Xiaoguang Wang [ID] *[ad]

Liquid crystal elastomers (LCEs) are a class of soft, stimuli-responsive materials that integrate the orientational order of liquid crystals with the elasticity of polymer networks. This molecular architecture imparts unique properties, including anisotropic actuation, reversible shape morphing, and programmable mechanical responses, which position LCEs as promising candidates for adaptive energy systems. Unlike rigid, static components, LCEs respond dynamically to external stimuli such as heat, light, and mechanical stress, allowing for autonomous and flexible energy transduction. Recent studies have highlighted the potential of LCEs in a range of energy applications, including solar energy harvesting and tracking, mechanical energy conversion, thermal energy regulation, and electrochemical energy storage. This Review examines recent advances in each of these four domains. Furthermore, key structure–function relationships, materials design strategies, and opportunities for system-level integration are discussed.

1. Introduction

Liquid crystal elastomers (LCEs) are a distinct class of soft, anisotropic materials that combine the orientational order of liquid crystals (LCs) with the elasticity of polymer networks.[1–6] Depending on the symmetry of molecular alignment, LCs can adopt nematic, smectic, or chiral nematic (cholesteric) phases,[1–11] where molecules align along a common director or form helical arrangements with periodic twist, as shown in Fig. 1(a). First conceptualized in the late 20th century, LCEs consist of mesogenic units covalently attached to or pendant from a crosslinked polymer backbone.[11,12] These mesogens can undergo thermotropic or photoinduced transitions between ordered (*e.g.*, nematic) and disordered (isotropic) states. When the mesogens are aligned within the polymer network, typically through external fields[13–17] or templated polymerization,[18–22] the material can deform in a programmable and reversible manner upon stimulation. This unique coupling between molecular order and macroscopic shape change underpins the key functionality of LCEs: reversible, stimuli-induced shape deformation. Upon thermal,[23–33] optical,[34–44] or other external cues,[45–49] the mesogens reorient or transition

between phases, driving anisotropic contraction, bending, twisting, or other complex shape transformations at the macro-scale. Unlike conventional actuators that rely on bulky components or rigid mechanisms, LCEs allow for untethered, soft actuation driven directly by changes in molecular orientation and entropy.

LCEs are typically synthesized through two coupled steps: (i) preparation of liquid crystalline polymers containing mesogenic units and (ii) crosslinking to form an elastomeric network. Depending on molecular architecture, LCEs are generally categorized as side-chain or main-chain systems (Fig. 1(b)).[50,51] In side-chain LCEs, mesogens are attached as pendants to a flexible backbone *via* alkyl spacers that decouple local LC order from the polymer chain motion. Main-chain LCEs, in contrast, incorporate the mesogenic units directly into the polymer backbone, which enhances coupling between LC alignment and mechanical strain. A variety of synthetic routes have been developed to construct such networks. The classical method introduced by Finkelmann employs a two-step hydrosilylation reaction between polyhydrosiloxane, vinyl-functionalized mesogens, and crosslinkers, allowing initial partial crosslinking and subsequent mechanical alignment before final curing.[52–56] This approach remains the benchmark for achieving monodomain LCEs with well-defined orientation. Other routes include step-growth polycondensation of mesogenic diols or diacrylates,[57–60] click chemistry between thiol and ene groups,[61–65] and photopolymerization of acrylate-functionalized mesogens.[66–69] The latter techniques allow spatial patterning of crosslinking density or orientation using light, facilitating complex or hierarchical director fields.

[a]William G. Lowrie Department of Chemical and Biomolecular Engineering, The Ohio State University, Columbus, OH 43210, USA. E-mail: wang.12206@osu.edu

[b]Department of Chemical and Biological Engineering, The Hong Kong University of Science and Technology, Clear Water Bay, Kowloon, Hong Kong, China. E-mail: yxyao@ust.hk

[c]School of Materials Science and Engineering, School of Physics, Georgia Institute of Technology, Atlanta, GA, 30332, USA. E-mail: shucong.li@mse.gatech.edu

[d]Sustainability Institute, The Ohio State University, Columbus, OH, 43210, USA

† Contributed equally to this work.

This journal is © The Royal Society of Chemistry 2026

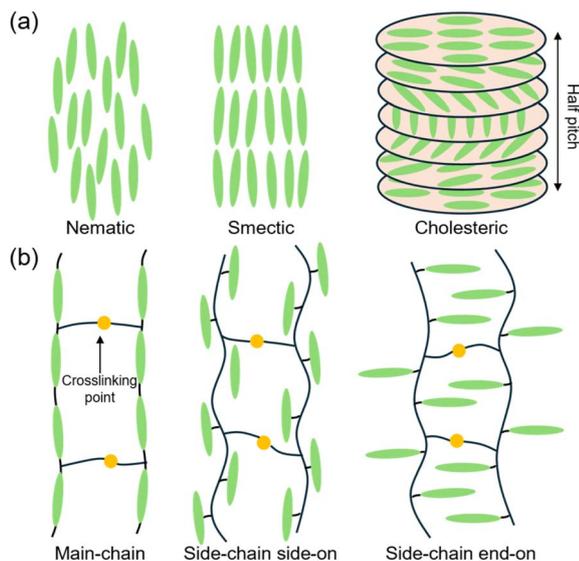*J. Mater. Chem. A*, 2026, **14**, 3185–3209 | **3185**

Fig. 1 Molecular order in LC mesophases and LCEs. (a) Schematic of LC molecular alignment in nematic, smectic, and cholesteric arrangements. (b) Structural representations of side-chain and main-chain LCEs.

Over the past decade, the energy materials field has increasingly recognized the potential of LCEs beyond actuation.[70–76] Their anisotropic molecular organization, mechanical adaptability, and responsiveness to multiple stimuli make them well-suited for emerging energy applications that demand dynamic, multifunctional material behaviour. In solar systems, LCEs allow autonomous light tracking, adaptive shading, and photothermal harvesting without external power or feedback control.[18,74,77] In electronics, their deformation-coupled conductivity and mechanical-to-electrical conversion open pathways to soft generators and piezoelectric/pyroelectric devices.[70,73,78] In thermal management, LCEs provide directional thermal conductivity, thermally responsive fabrics, and elastocaloric cooling under low stress.[18,19,48,54] Finally, in energy storage systems, LCE-based electrolytes and shape-morphing devices offer promising solutions for deformable and reconfigurable platforms.[45,55–59]

We acknowledge that several comprehensive reviews have already addressed liquid crystalline materials in energy applications, including smart windows,[79–83] adaptive solar unfolding system,[84] and radiative-cooling materials.[85] In contrast to these reviews, this Review discusses how the mesogen alignment, polymer network topology and macroscopic shape change in LCEs enable their application across four energy domains (solar, electrical, thermal and electrochemical). For each area, we highlight material design strategies, shape deformation mechanisms linking structure and function, and device-level demonstrations, and identify current limitations and future directions. Overall, this Review emphasizes a unified structure–property–function perspective and aims to provide a roadmap for integrating LCEs into adaptive, responsive energy systems.

2. LCEs for solar energy applications

Solar energy applications typically refer to technologies that convert sunlight into usable forms of energy, such as thermal, electrical, or mechanical energy. This broad category includes photo-activated actuators,[86–88] photovoltaic systems,[89–91] solar thermal collectors,[92,93] and light-regulating energy-efficient architectural elements.[68,69,94–96] These systems aim to harness the abundant and renewable energy from the sun to power devices, prevent environmental pollution from fossil fuels, and increase energy efficiency in a variety of applications. LCEs are increasingly recognized as stimuli-responsive materials for solar energy systems due to their intrinsic photothermal responsiveness and shape programmability. Understanding of photo-actuation behaviour in LCEs will be helpful for the comprehension of subsequent applications.

For photo-chemical–mechanical actuation, photo-activated trans–cis isomerization in azobenzene,[97–99] spiropyrans derivatives,[100,101] and donor–acceptor Stenhouse adduct (DASA)[102,103] has been widely used to generate local free volume at molecular level. This isomerization further leads to mechanical deformation (such as bending, twisting, or expansion) at the macroscale. These effects ultimately result in a decrease in density, a softening of the modulus, and the generation of stress and strain, respectively. Potential applications include actuators,[34,62,76,88] soft robotics,[104,105] artificial muscles,[106–108] and smart interfaces,[109–112] where precise, remote-controlled deformation is essential for responsive and adaptive functionality. In photothermal mechanisms, the absorption of light by the LCEs themselves or photothermal agents (e.g., gold nanoparticles,[113] carbon nanomaterials,[114] and organic dyes[115]) results in a localized temperature increase. This heating then triggers phase transition (for instance, nematic to isotropic) causing shape deformation. This mechanism holds promise for use in dynamic glazing technologies, solar trackers, and other light-responsive systems that require autonomous adjustment to varying sunlight conditions. Photonic bandgap shift in cholesteric or inverse opal LCEs is a light-responsive mechanism where structural changes in the LCE mesogen lead to dynamic modulation of optical properties.[116–118] After exposure to external stimuli (such as light or heat), LCEs undergo anisotropic deformation, which alters the periodicity or pitch of the photonic structure.[118,119] This deformation results in a shift of the photonic bandgap, visibly manifested as a reversible colour change. Such behaviour opens the door to applications in tunable photonic devices,[120,121] smart windows,[122,123] and mechanochromic sensors,[124] where visual feedback or wavelength control is required. Additionally, electrical energy can be generated based on photothermal or photomechanical mechanisms, as seen in solar harvesting. As researchers continue to explore these functions, LCEs have been proved to be a powerful platform for developing responsive and multifunctional solar energy technologies. This section will discuss applications of photoresponsive LCEs in several innovative areas, including photo-activated actuators, optical modulation in solar cells, and smart windows. Notably, several of the studies rely on UV light as the activation source, owing to the conventional photochromic molecules (such as

3186 | J. Mater. Chem. A, 2026, 14, 3185–3209

This journal is © The Royal Society of Chemistry 2026

azobenzene) that are primarily UV responsive. We have clarified the light source used in these examples to avoid potential confusion.

2.1. Solar energy-driven LCE actuators

Conventional solar energy-driven actuation systems often rely on rigid components,[124] external power sources,[125] or static geometries[126] that limit their flexibility, responsiveness, and integration with soft or curved surfaces. Based on light-triggered mechanisms listed above, LCEs have become one of the most promising candidate materials to address challenges by combining light-sensitive molecular alignment with elastic polymer networks. As photoresponsive actuators, LCEs can convert light into mechanical motion through two primary mechanisms: photochemical conversion, which generates local free volume and induces macroscopic deformation *via* molecular isomerization,[127–130] and photothermal conversion, where absorbed solar energy is transformed into heat.[131–135] In the latter case, this thermal energy transformation is often enhanced by doping with photothermal agents such as polydopamine, gold nanorods and carbon nanotubes, leading to phase transitions and subsequent mechanical actuation.[136,137] These mechanisms allow soft, autonomous actuation in response to light without the need for motors or electronic controllers. By controlling molecular alignment through techniques such as mechanical rubbing,[138] photoalignment,[139] or patterned crosslinking,[140] these systems achieve precise and reversible deformation. Their soft, lightweight, and programmable nature makes LCEs especially suitable for next-generation solar energy applications requiring shape adaptability and material intelligence.

These approaches have permitted the design of programmable, solar-powered actuators capable of complex motion, making LCEs attractive for artificial muscles, soft robotics, and biomimetic devices. Lewis *et al.* developed a 3D-printable LCE ink with dynamic covalent bonds that enable reversible, programmable shape changes.[141] As shown in Fig. 2(a), the printed structures deform upon heating through the LCE phase transition, and subsequent UV exposure locks the shape *via* dynamic bond exchange. This method supports permanent fixing of temporary shapes and reconfiguration into complex, heterogeneous 3D architectures.

Furthermore, Chen *et al.* translated the nanoscale rotation of molecular motors into macroscopic motion by integrating unidirectionally rotating photoresponsive moieties into 3D-printed LCEs.[104] Upon UV irradiation, the embedded motors generate rapid and directional deformation, allowing for layered assemblies with preprogrammed, biomimetic functions (Fig. 2(b)).

Wei *et al.* fabricated scalable, multi-responsive LCE fibres by incorporating a polydopamine-modified MXene (PDA@MXene) coating.[142] The composite fibres exhibit enhanced photothermal response and stable electrical conductivity. When actuated by near-infrared (NIR) light, the fibres generate large, rapid, and reversible contractions and can lift weights over 1000 times their own mass (Fig. 2(c)).[142]

Schenning *et al.* have reported a LCE polymer film doped with a fluorinated azobenzene (F-azo) which exhibits continuous chaotic oscillation under ambient sunlight.[145] Unlike conventional actuators requiring modulated light, this system self-oscillates under constant illumination. The motion arises from the simultaneous exposure to blue and green light, driving reversible photoisomerization of azobenzene. This polymer film demonstrates reversible, sunlight-powered actuation without external control, as shown in Fig. 2(d).

Ikeda *et al.* have presented a pioneering study on a light-driven plastic motor based on azobenzene containing LCEs (shown in Fig. 2(e)), which utilize the reversible *trans–cis* photoisomerization of azobenzene under UV and visible light, inducing localized contraction and expansion in polymer layer.[143] By laminating the LCEs with a flexible polyethylene sheet, the composite layer can achieve photo responsiveness with outstanding mechanical durability at the same time. When setting up with a belt and mounted on pulleys, the films rotate continuously under UV and visible light irradiation, converting light energy into mechanical motion directly.

Broer *et al.* reported a LCE polymer film incorporating fast-relaxing azobenzene derivatives that exhibits continuous mechanical wave propagation under constant light illumination.[39] Different with conventional photo actuators requiring modulated stimuli, this system generates directional travelling waves through a self-shadowing feedback mechanism. In this system, the film features a splay-aligned molecular configuration, enabling reversible bending upon UV exposure. When clamped at both ends and illuminated unidirectionally, the film undergoes perpetual wave motion, for which direction can be controlled by its planar or homeotropic side orientation (Fig. 2(f)).

2.2. LCEs for solar tracking and light concentration

Optical modulation in solar cells involves dynamically adjusting how sunlight is directed, focused, or distributed across the photovoltaic surface to enhance overall energy harvesting efficiency. Traditional solar systems rely on static optical elements[126] or mechanical tracking mechanisms to maintain optimal light incidence,[144] which increases cost and limits adaptability. One of the main challenges is achieving efficient, real-time solar tracking or light shaping without relying on motors or external control systems. LCEs offer a novel solution with their ability to autonomously deform toward a solar source when exposed to light. When engineered into reconfigurable lenses or alignment-based optical layers, LCEs can bend or reshape to follow the sun's movement or alter light paths, optimizing illumination on solar cells. In addition, the shape deformability and anisotropic optical properties of LCEs allow them to control light polarization and transmission, further enhancing the performance of advanced photovoltaic architectures.

Inspired by natural plant heliotropism, Jiang *et al.* reported a novel LCE nanocomposite system designed to autonomously orient toward sunlight, mimicking the natural heliotropic behaviour of plants, as shown in Fig. 3(a).[74] This behaviour is
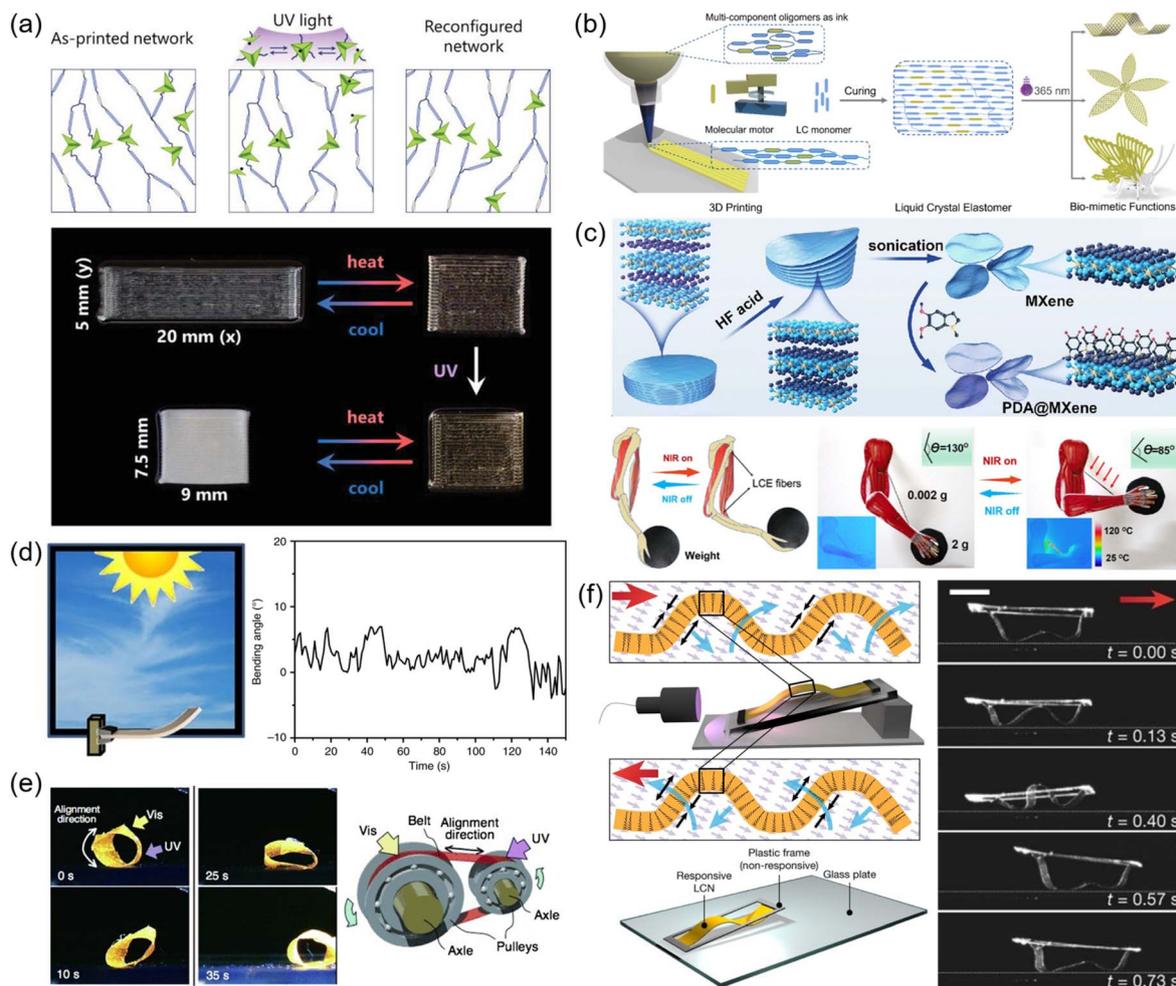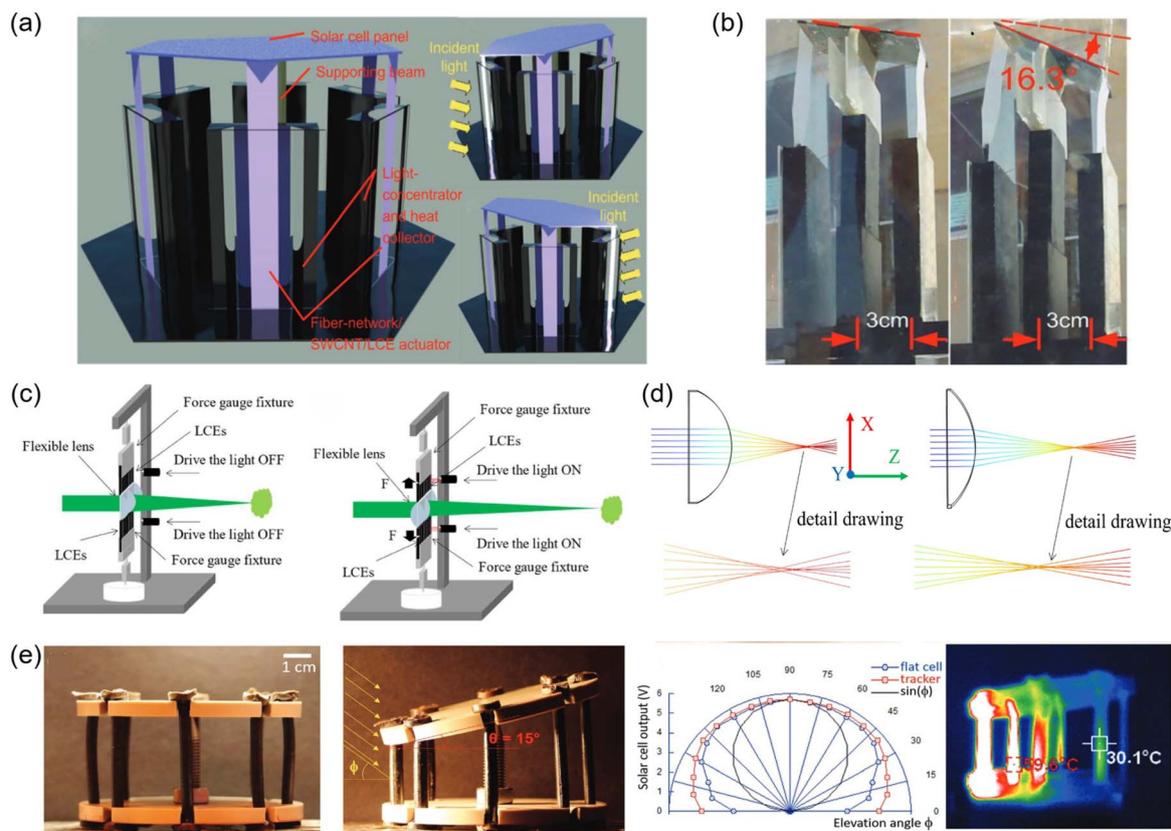
Fig. 2 Multifunctional LCE actuators: fabrication strategies, stimuli responses, and programmable deformations. (a) HOT-DIW printing of reconfigurable LCEs with light-induced shape memory. Top: schematic of LCE networks in the as-printed state, during UV-triggered dynamic bond exchange, and after fixation into a permanent shape. Bottom: optical images showing thermally reversible actuation and shape fixing after UV exposure, including patterned actuation and localized reconfiguration using photomasks. Reproduced with permission.[141] Copyright 2019, John Wiley and Sons. (b) Photoresponsive biomimetic functions of 3D-printed LCEs with covalently integrated light-driven molecular motors. Preprogrammed printing paths yield morphologies such as bilayer flowers and butterfly wings, enabling bending, helical coiling, petal closure, and wing flapping under light. Reproduced with permission.[104] Copyright 2024, American Chemical Society. (c) Preparation and actuation of PDA@MXene-integrated LCE fibre actuators (top) and NIR-driven muscle-mimetic actuation (bottom). Reproduced with permission.[142] Copyright 2014, Royal Society of Chemistry. (d) Continuous chaotic oscillations of *ortho*-fluoroazobenzene polymer film in sunlight. Right: plot of the bending angle as a function of time when F-azo polymer film exposed to solar simulator.[143] Copyright 2016, Springer Nature. (e) Photoinduced rolling motion of a continuous ring of LCE film. Series of photographs on the left show time profiles of the photoinduced rolling motion of the LCE ring by simultaneous irradiation with UV and visible light. On the right is the schematic illustration of the light-driven plastic motor system used in this study. Copyright 2008 Johns Wiley and Sons. (f) Schematic illustration of experimental set-up, showing a polymeric film that is constrained at both extremities under an oblique-incidence light source (left). Blue arrows show the way the film deforms while the red ones indicate the propagation direction of the wave. Right: the motion of polymer films with the planar side up fixed to a passive frame. Red arrows here indicate the direction of motions. The dashed line represents the top surface of the glass plate.[144] Copyright 2017 Springer Nature.

achieved by integrating photothermal nanoparticles (*e.g.*, carbon black and gold nanorods) into the LCE matrix, which allows for efficient solar light absorption and localized heating. Upon exposure to sunlight, the photothermal effect raises the local temperature, inducing the nematic-to-isotropic phase transition in the LCE and driving directional bending. As sunlight hits at different angles throughout the day, differential heating across the LCE structure continuously reorients the actuator toward the sun without any need for external sensors,

motors, or power inputs, as shown in Fig. 3(b).[74] The system demonstrates high responsiveness, reversible actuation, and precise sun-tracking capability, and its simplicity and autonomy make it particularly attractive for use in solar concentrators, light-redirecting devices, or low-power solar tracking systems.

Jiang *et al.* presented an artificial heliotropism based on LCEs that enables solar cells to automatically track the light source under NIR light stimulation without external power, as illustrated in Fig. 3(c).[146] The core of this technology is a novel

3188 | *J. Mater. Chem. A*, 2026, **14**, 3185–3209

This journal is © The Royal Society of Chemistry 2026

Fig. 3 Light-driven LCE actuator system for solar tracking and optical energy harvesting. (a) Schematic of artificial heliotropism.[74] (b) Field demonstration of a dual-LCHC actuator device and photocurrent enhancement from a single unit. Reproduced with permission.[74] Copyright 2012, John Wiley and Sons. (c) Light-responsive LCE-actuated variable-focus cylindrical lens in initial and illuminated states.[146] (d) Ray diagram illustrating focal length tuning of the LCE-based lens. Reproduced with permission.[146] Copyright 2025, Optica Publishing Group. (e) Photographs of an LCE-actuated passive solar tracking device in its initial and sunlight-tilted states (top) and polar plot of solar cell output versus elevation angle for flat and tracking configurations, and infrared thermal image showing actuator heating (bottom). Reproduced with permission.[94] Copyright 2021, John Wiley and Sons.

photothermal-mechanical system, consisting of an LCE matrix integrated with single-wall carbon nanotubes and reinforced with a polyurethane fibre-network. When the actuator is exposed to sunlight, single-wall carbon nanotubes convert light into heat, causing the LCEs to contract. This contraction pulls on the platform equipped with solar cells, tilting the system towards the sun and thus enhancing efficiency. The NIR light serves as a remote, localized stimulus, making the lens suitable for integration with solar concentrators and optical tracking systems. The ability to precisely tune the lens' focus in response to environmental light conditions could improve energy efficiency in solar panels by optimizing light capture and distribution, as shown in Fig. 3(d).[146] By programming the LCE's molecular alignment, the lens undergoes anisotropic deformation upon NIR exposure, allowing for real-time and reversible changes in curvature. This tunable optical behaviour addresses the need for adaptive light modulation in solar energy systems. The LCE-based lens offers several advantages over traditional optical elements, such as being flexible, lightweight, and capable of autonomous shape adjustment without motors or mechanical parts.

Similar to Jiang et al.'s work,[74] Terentjev et al. have developed a helio-tracking device that can mimic the phototropism of plants, like sunflowers, to autonomously track a light source, as shown in Fig. 3(e).[94] This device features a freely pivoting platform supported by linear actuators made from photoresponsive exchangeable LCEs. These LCEs, synthesized using click chemistry, contained indocyanine green dye, which can absorb broad-spectrum light and realize a photothermal effect. In experimental tests, the device achieved a stable 15° tilt and increased total energy output of an attached solar cell by 10% compared to a fixed one. Overall, these results highlight how LCEs can be used as highly controllable, reconfigurable optics in solar energy applications, which provides a promising step toward fully soft, adaptive solar systems. Here, Table 1 summarizes the representative materials used in photo-mechanical materials for actuators, including LCE-based system, amorphous polymers, shape memory polymer composite and molecular crystals. This table makes a comparison of their mechanisms and key metrics in photo-mechanical conversion (such as mechanical strain, response speed) and highlights the advantages and limitations for each materials system. LCEs have been considered as an ideal material due to

This journal is © The Royal Society of Chemistry 2026

J. Mater. Chem. A, 2026, 14, 3185–3209 | 3189

Table 1 Comparison of photo-responsive material systems for actuation

Material system	Photo-actuation mechanism	Photo-actuation mechanical strain	Response speed	Key advantages of LCEs	Limitations and challenges	Ref.
LCE-based system	Photo-chemical; photo-thermal	20–60%	ms–s	Reversible deformation; programmability; photo-chemical: fast response and spatiotemporal control; photo-thermal: large strain output and broad selection of responsive wavelength	Photo-chemical: small strain output; limited penetration depth; limited selection of responsive wavelength; photochemical fatigue. Photo-thermal: poor spatial control	39 and 147–149
Amorphous polymers	Photo-chemical	~1%	s–min	Easy fabrication and processing; broad materials selection	Small strain output; slow response; uncontrollable deformation; low efficiency	150–153
Shape-memory polymer composite	Photo-thermal	up to >100%	s–min	Large strain amplitude; abundant processing methods	Slow response; limited cycle lifetime; low efficiency; poor spatial control	154–156
Molecular crystals	Photo-chemical	15–40%	μs–ms	Extremely fast response; high modulus; outstanding fatigue resistance for specific molecules	Limited strain output; brittle; difficult to process; limited selection of responsive wavelength	157–160

their fast response, reversibility and programmability as actuator in many applications while other materials cannot maintain these advantages at the same time.

2.3.   LCEs for adaptive smart window technologies

Smart windows are glazing systems or coatings that can dynamically adjust their optical properties such as light transmission, shading, or transparency in response to environmental stimuli like sunlight, temperature, or voltage.[122,161–163] Their goal is to control the amount of solar radiation entering a building to reduce reliance on heating, cooling, and artificial lighting systems, thereby improving energy efficiency and indoor comfort. Current challenges in smart window technologies include limited responsiveness, slow switching speeds, and high energy consumption in electrically driven systems.[164] Many existing systems also lack autonomous behaviour and require complex wiring or power supply systems. LCEs offer an innovative solution due to their ability to deform or alter optical properties in response to heat or light. When used as thin films in smart windows, LCEs can change shape, curvature, or alignment to modulate light scattering, reflection, or transparency without external power input.[165–169] Their photothermal responsiveness permits adaptive control of window function based on solar intensity, and their flexibility allows easy integration into both flat and non-planar architectural surfaces. Moreover, the anisotropic optical nature of LCEs allows for precise tuning of polarization and light direction, supporting multifunctional window systems.

Schenning *et al.* introduced a smart window based on twisted nematic LCE films, which modulate light reflection in response to ambient temperature changes. The core innovation lies in the use of a polymer-stabilized twisted nematic LC configuration that can switch between reflective and transparent states without electrical input, as shown in Fig. 4(a).[165] As the temperature crosses a threshold the alignment of the LC

moieties shifts, altering the optical path and reflectivity of the film. As a result, these reflective LCE windows can autonomously reduce solar heat gain in buildings, contributing to passive cooling. The optical response is reversible, fast, and does not require continuous power, making it advantageous for sustainable building integration. This work demonstrates how orientational order of LCEs can be engineered for climate-responsive architecture, offering pathways for smart light-regulating window systems.

Recently, there has been growing interest in developing smart windows that respond to multiple stimuli to improve energy efficiency. LC systems have shown notable potential for applications in energy-efficient buildings. Jiang *et al.* reported an innovative LC-based smart window system that autonomously adjusts its transparency in response to both environmental temperature and light intensity, as shown in Fig. 4(b).[170] This system incorporates isobutyl-substituted diimmonium borate, which is transparent in the visible spectrum but can convert NIR light into heat efficiently. When doped in a chiral LC matrix, the system can dynamically adjust its transparency, reflectivity, and thermal insulation in response to changing environmental conditions. This muti-stimuli responsiveness allows the window to switch modes, such as shading under strong sunlight or light diffusion under overcast conditions. We comment here that although this system focuses on LC rather than LCE, the photothermal mechanism is fundamentally similar: light absorption generates localized heating that triggers a phase transition and alters optical properties. This example demonstrates how analogous photothermal processes in LCEs can drive light-induced phase transitions, achieving adaptive and responsive behavior in smart window. In contrast to conventional smart windows that respond to a single stimulus, this integrated design broadens functional versatility and operational applicability under diverse environmental conditions.

For LCE systems, Yao *et al.* developed a method to create dynamic wrinkled patterns on the surface of LCEs, as seen in
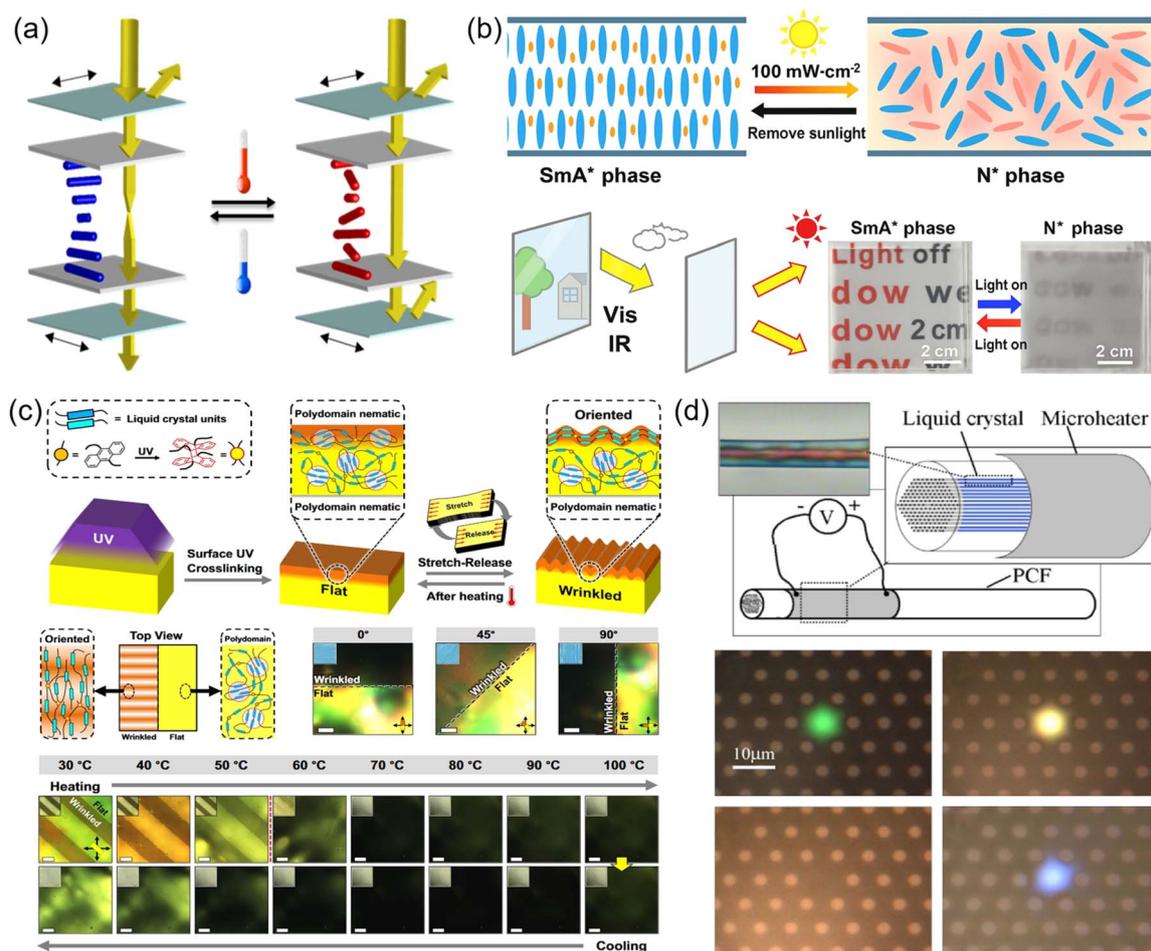
3190 | *J. Mater. Chem. A*, 2026, **14**, 3185–3209

This journal is © The Royal Society of Chemistry 2026

Fig. 4 Thermally and optically responsive LC systems for tunable optics, smart windows, and surface reconfiguration. (a) Reflective smart window with polarization-selective elements (black arrows: polarization direction; yellow arrows: light path). Reproduced with permission.[165] Copyright 2021, John Wiley and Sons. (b) Photothermal dual-passive LC smart window: schematic and experimental demonstration. Reproduced with permission.[170] Copyright 2022, American Chemical Society. (c) Schematic of the mechanism underlying dynamic surface wrinkling (top), top-view model and corresponding molecular alignment in wrinkled (UV-exposed) and flat (unexposed) regions (middle), and polarized light micrographs showing alternating wrinkled and flat regions during heating–cooling cycles (bottom). Reproduced with permission.[171] Copyright 2024, Springer Nature. (d) Photonic crystal fibre device with microheater and LC-filled core (top) and temperature-tuned colour changes from photonic bandgap shifts (bottom). Reproduced with permission.[172] Copyright 2003, Optical Society of America.

Fig. 4(c).[171] When exposing the anthracene-containing LCE film to UV light, it forms a stiff, gradient-crosslinked top layer. The subsequent stretching and releasing cycles induce buckling due to a modulus mismatch between the stiff surface and soft interior, resulting stable wrinkles. The ability to switch the surface from a flat, transparent state to a wrinkled, light-scattering state provides a mechanism for tunable transparency, which brings the system potential to be utilized in energy-efficient buildings. In addition to surface and alignment-based strategies, photonic bandgap engineering offers another promising pathway for light-regulating smart windows.

Broeng *et al.* demonstrated how infiltrating LCs into photonic crystal fibre structures enables dynamic control over light transmission, as shown in Fig. 4(d).[172] In this system, external stimuli such as temperature or light alter the refractive index and molecular alignment of the LC core, resulting in tunable photonic bandgap behaviour. This behaviour allows for

reversible modulation of transmitted wavelengths with high optical contrast and no electrical input. The underlying mechanism highlights how LC-based photonic structures can be adapted into flat or film-based LCE systems for smart window applications. Such materials could autonomously regulate solar heat and light transmission through controlled bandgap shifts, offering a novel strategy for the development of passive, programmable, and energy-efficient window technologies.

2.4. Challenges and opportunities

Although many LCEs reported in this field still rely on UV light as the activation source, emerging strategies aim to shift their responsiveness toward visible and NIR light, expanding their applicability for solar-driven actuation and energy-harvesting applications.

The above studies demonstrate that LCEs and LC-hybrid materials offer distinct advantages for solar applications,

This journal is © The Royal Society of Chemistry 2026

J. Mater. Chem. A, 2026, **14**, 3185–3209 | **3191**

including autonomous actuation, mechanical flexibility, low energy input, and the ability to harvest energy from light. Despite this promise, several critical challenges remain. First, the energy conversion efficiency of both photochemical and photothermal systems requires further development, particularly in effectively translating nanoscale molecular motion or localized heat into macroscopic mechanical work. In addition to the inefficient energy transduction, conventional photochromic molecules can only adsorb in limited wavelength range, restricting the solar light utilization. Potential strategies include designing molecules to extend the adsorption spectrum to visible light and NIR region by expanding the π-conjugation of azobenzene groups or incorporating donor–acceptor substituents.[173] Second, scalable fabrication methods are lacking; bridging the gap between lab-scale demonstrations and practical deployment will require new synthetic strategies and efficient, robust processing techniques for producing photoresponsive LCEs. Developing suitable LCEs inks offer a promising route towards continuous and large-area fabrication.[174–176] Third, long-term durability and fatigue resistance under operational conditions remain challenging. Photochemical systems are prone to photodegradation, while photothermal systems may degrade under sustained thermal cycling or mechanical strain. Incorporating dynamic covalent chemistry into the LCE network, in which energy can be dissipated locally and self-repair through reversible bond exchange, further improve materials lifetime.[177] In addition, poor light absorption under low-intensity sunlight can be mitigated by designing light-trapping microstructures (such as porous structures) that enhance the optical path length.[178] Nevertheless, difficulties in achieving uniform molecular alignment over large areas, along with limited stability under prolonged UV exposure and temperature fluctuations further constrain real-world implementation.

3. Electronic applications in LCEs

In recent years, LCEs have attracted growing attention for their potential in charge transport and electricity generation applications due to their well-controlled molecular packing and so-induced mechanical properties.[18,78,179,180] Owing to their intrinsic anisotropy in molecular packing,[181,182] LCEs facilitate directional charge transport.[18] Moreover, such molecular anisotropy can introduce mechanical deformations driven by phase transitions. These deformations can be coupled with mechanical-to-electrical energy conversion mechanisms to transduce various forms of energy into electrical energy.[78,179,183] Such energy conversion ability of LCEs offers promising opportunities for energy harvesting and the development of self-powered systems.[184]

3.1. Charge transport in LCEs

Efficient and stable charge transport is a key requirement for high-performance flexible devices.[185,186] Currently, the development of most soft materials focuses on molecular design to balance mechanical compliance and intrinsic charge carrier

mobility. The molecular packing of such charge-transporting molecules is less studied due to its difficult implementation,[187,188] even though the conductivity of semiconductive polymers has been demonstrated to be significantly improved through macroscopic alignment of functional molecules. LCEs offer a versatile and easy-to-complement platform to achieve such large-scale alignment, with their ordered mesogenic domains facilitating directional charge transport.

Using the ordered molecular alignment of LCEs, researchers have integrated them into perovskite solar cells (PSCs) to enhance charge transport performance. For one example, Song et al. used LCE as functional interlayer in PSCs, effectively directing the formation of ordered and efficient charge transport pathways between the perovskite absorber layer and the electron transport layer (Fig. 5).[18] The ordered LCE interlayer enhanced charge transport through multiple effects: first, its incorporation shifts the conduction band minimum of the interlayer closer to that of the perovskite, thereby improving energy level alignment, which in turn facilitates more efficient electron injection. Second, they induce negligible surface potential difference, which contributes to the formation of more uniform charge transport pathways across the interface. Third, the ordered LCE interlayer significantly reduces the trap-filling limit voltage, suppressing trap density by nearly an order of magnitude and simultaneously passivating unsaturated Pb^{2+} sites through sulfur–lead interactions, which collectively contribute to its effective surface passivation capability.[50] These benefits translated into substantial device performance improvements: rigid PSCs incorporating LCEs achieved a power conversion efficiency (PCE) of 23.26%, while flexible PSCs reached 22.10%. These findings demonstrate the broader potential of LCEs in electronics, where their unique combination of molecular order and mechanical adaptability can enable the development of high-performance energy devices.

3.2. Electricity generation in LCEs

As discussed earlier, LCEs exhibit reversible mechanical deformation in response to external stimuli such as heat,[189] light,[190,191] or humidity.[192] This dynamic behavior can be used to generate electricity when coupled with piezoelectric[193,194] or electromagnetic induction mechanisms.[195–198] In piezoelectric energy harvesting, the stimuli-responsive actuation of LCEs serves as an internal mechanical stress generator. For example, Yang et al. demonstrated that thermally triggered mechanical
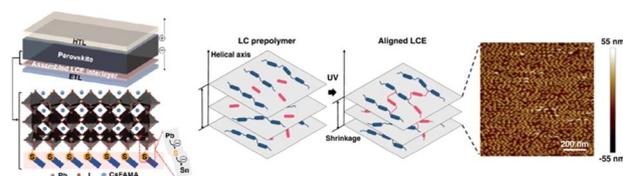

Fig. 5 Integration of aligned LCE interlayer in perovskite solar cells. Schematic of device structure with LCE layer formed via photopolymerization of oriented LC prepolymer. Reproduced with permission.[18] Copyright 2023, Springer Nature.
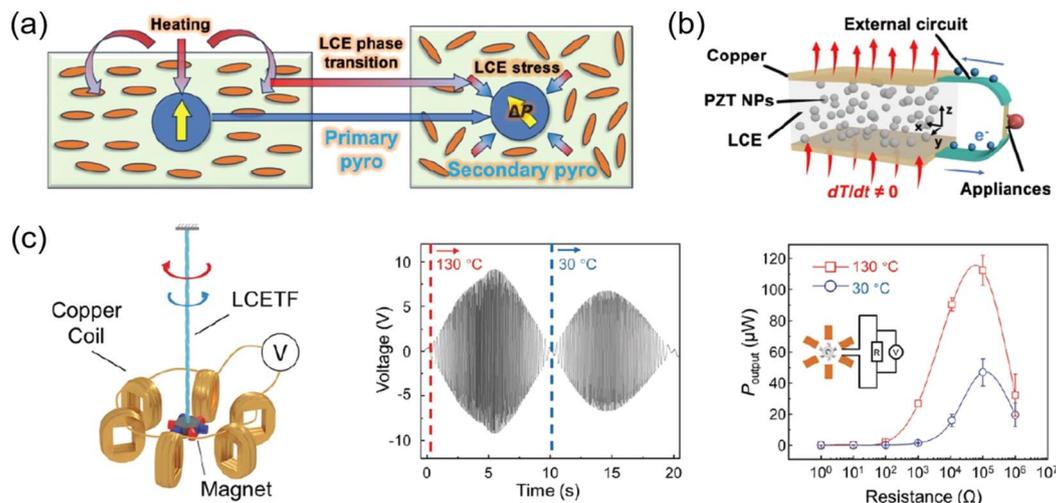
3192 | J. Mater. Chem. A, 2026, **14**, 3185–3209

This journal is © The Royal Society of Chemistry 2026

Fig. 6 Pyroelectric and thermomechanical energy harvesting in LCE-based transducers. (a) Pyroelectric enhancement *via* piezoelectric coupling in LCE/PZT composites under mechanical stress.[180] (b) Schematic of LCE/PZT harvester. Reproduced with permission.[180] Copyright 2025, The American Association for the Advancement of Science. (c) Thermally activated LCETF generator: open-circuit voltage from 130 °C to 30 °C and output power *versus* load resistance. Reproduced with permission.[195] Copyright 2022, John Wiley and Sons.

stress in LCEs can deform piezoelectric materials to generate electric bias.[180] Compared to current thermal-electrical energy conversion based solely on the pyroelectric effect (where temperature variations directly modulate polarization, producing electric displacement),[193] the additional incorporation of the piezoelectric effect in this system yields significantly improved energy conversion performance.[78,179]

Building on this approach, Yang *et al.* further developed LCE/lead zirconate titanate (PZT) composites by embedding piezoelectric PZT nanoparticles into the LCE matrices.[180] As shown in Fig. 6(a) and (b),[180] the LCE matrix undergoes thermal expansion or contraction, transmitting stress to the PZT phase and thereby inducing a strong piezoelectric response. This synergy between LCE actuation and piezoelectric transduction led to a total pyroelectric coefficient of $p = -4.01$ nC cm^{-2} K^{-1}, exceeding the values reported for other flexible pyroelectric materials (*e.g.*, PDMS/KNbO$_3$ nanowire at -0.80 nC cm^{-2} K^{-1},[199] PVA–PAA/PZT at -2.85 nC cm^{-2} K^{-1},[200] and even the highest-performing polyvinylidene fluoride (PVDF) variants at -3.00 nC cm^{-2} K^{-1} (ref. 201–203)). These results highlight the potential of LCE-based hybrid systems to advance soft, thermally responsive energy generators through mechanically mediated energy transduction.

The exceptional structural design flexibility of LCEs, combined with their reversible, stimulus-responsive mechanical properties, allows for various types of deformations, such as contraction and bending.[27,204] These dynamic motions can be exploited in electromagnetic induction systems, where electricity is generated through relative motion between a magnet and a coil. To leverage this principle, Yang *et al.* developed LCE twist fibers (LCETFs) by chemically crosslinking pre-aligned twisted mesogens.[195] Upon thermal stimulation, the LCETFs exhibit significant torsional motion, achieving up to 31% axial contraction (Fig. 6(c)).[195] This actuation is fully reversible, with the fibers returning to their original state upon cooling,

allowing for continuous bidirectional rotation across heating–cooling cycles. This reversible torsional motion was harnessed to rotate a magnet around a copper coil, inducing a voltage output of 9.4 V and a peak power of 120 μW *via* electromagnetic induction. This corresponds to a power density of 6 W kg^{-1}, comparable to the average output of a competitive cyclist. Beyond power generation, LCETFs demonstrated superior performance compared to commercial motors and conventional materials, achieving a specific torque of 10.1 N m kg^{-1}, energy density of 115.3 kJ m^{-3}, and a torsional strain of 243.6° mm^{-1}. These results highlight LCETFs as a promising platform for soft, thermally driven energy harvesters and actuators in next-generation robotics and wearable systems.

3.3. Challenges and opportunities

Despite the significant potential of LCEs in charge transport and electricity generation, several challenges remain. For instance, the intrinsic charge mobility of LCEs is relatively low and heavily dependent on molecular order, which is difficult to preserve during device fabrication. Additionally, current energy conversion efficiencies require further enhancement. Nevertheless, the unique flexible architecture, multi-stimuli responsiveness, and integration potential of LCEs offer valuable opportunities for the development of next-generation intelligent, self-powered systems, flexible sensors, and environmental energy harvesters. Future research may benefit from optimizing molecular design. For example, introducing highly conjugated aromatic ring units derivatives to enhance π–π stacking and promote charge transport, regulating persistence length and Kuhn length of LCE molecular chains to enhance chain rigidity, thereby improving stress transfer efficiency during deformation, and regulating cross-linking density to optimize LCE's deformation amplitude and response speed. In addition, it should focus on regulating multi-field coupling mechanisms

This journal is © The Royal Society of Chemistry 2026

J. Mater. Chem. A, 2026, **14**, 3185–3209 | **3193**

Table 2 Performance of LCE-based electronic components

Material functions	Performance	Key advantages of LCEs	Limitations and challenges	Ref.
Anisotropic charge transport (3.1)	Absolute resistance: SnO_2/LCE: $R = \sim 10\ \Omega$ vs. SnO_2/3-aminopropyl triethoxysilane: $R = \sim 14.3\ \Omega$	Directional charge transport, compatibility with flexible devices	Low intrinsic charge mobility	18
	Conductivity: LCE composites 10^{-3}–10^3 S cm^{-1} vs. traditional ion-conductive polymer composites 10^{-5}–10^0 S cm^{-1}			205–209
Electricity generation through mechanical deformations (3.2, 3.3)	Through pyroelectric effect: pyroelectric coefficient: LCE/PZT $p = -4.01$ nC cm^{-2} K^{-1} vs. flexible pyroelectric materials $p = -0.8$ to -3.00 nC cm^{-2} K^{-1}	Superior energy conversion to single effects (enhanced pyroelectric coefficient)	Sophisticated material integration	180 and 210–214
	Through electromagnetic induction: specific torque: LCE 10.1 N m kg^{-1} vs. commercial electric motors 6.0 N m kg^{-1}	Flexible, integrating power generation and actuation	Insufficient response speed	195 and 215

and advancing system-level integration to transition LCEs from fundamental studies to real-world applications. Table 2 summarizes the reported performance metrics of LCE-based electronic components.

4. LCEs for thermal energy management

Thermal management technology aims to control temperature in applications such as preventing electronic devices from overheating, regulating cabin temperature in electric vehicles, managing heat flow in solar panels, or maintaining optimal temperatures for biomedical implants.[216] LCEs, with their anisotropic molecular alignment and stimulus-responsive deformation, offer a unique platform for active thermal control. Controlled molecular alignment contributes to their anisotropic thermal conductivity, allowing for directional heat control (Fig. 7(a)).[217] In addition, micro- and macroscopic mechanical deformations in LCEs can achieve thermal regulation in smart textiles.[218,219] These properties make LCEs promising for applications such as directional heat dissipation, thermally adaptive textiles, and energy conversion.

4.1. LCEs for anisotropic thermal conductivity

Efficient thermal management materials must facilitate directional and fast heat transfer from heat sources to heat sinks and minimize interfacial thermal resistance.[222] LCEs have recently emerged as a new class of thermally conductive polymers due to their intrinsic anisotropy. This molecular-level anisotropy allows heat to be preferentially conducted along the direction parallel to molecular alignment and suppress thermal diffusion in perpendicular directions (Fig. 7(b)).[220] This behavior arises from anisotropic phonon transport:[221] the alignment of mesogens facilitates continuous molecular pathways[223] and reduces

phonon scattering by minimizing chain entanglements and defects.[224,225] In particular, the suppression of grain boundaries, which are common in disordered polymers, further lowers interfacial phonon scattering and enhances thermal transport along the alignment direction. In contrast, perpendicular to the alignment, looser packing and disrupted molecular continuity introduce more frequent scattering events, significantly compromising heat transfer efficiency (Fig. 7(c)).[221]

4.2. Directional heat dissipation in high-frequency electronics

With the rapid miniaturization and integration of modern electronic devices such as 5G and wearable systems, efficient thermal management of high frequency operations has become a bottleneck limiting device performance and lifespan.[226,227] Conventional isotropic polymer coatings exhibit intrinsically low thermal conductivity due to disordered molecular chain arrangements.[228] In contrast, LCEs maintain thermal conductivity anisotropy even under strain, due to collective mesogen alignment and soft elasticity. Fytas et al. demonstrated that LCEs retain stable phonon group velocity under deformation, achieving consistent heat dissipation at GHz frequencies (Fig. 8).[229] This capacity to direct heat along predefined axes without compromising mechanical compliance makes LCEs especially suitable for thermal management in flexible and high-frequency electronics.

4.3. LCE-based fabrics for adaptive thermal insulation

Thermally responsive LCEs offer a compelling approach to smart textiles that interact intuitively with biological systems. By tuning the phase transition temperature of LCEs to fall within the range of human physiological conditions, researchers have created materials that respond directly to body heat.[230] These transitions drive controlled shape morphing

3194 | J. Mater. Chem. A, 2026, 14, 3185–3209

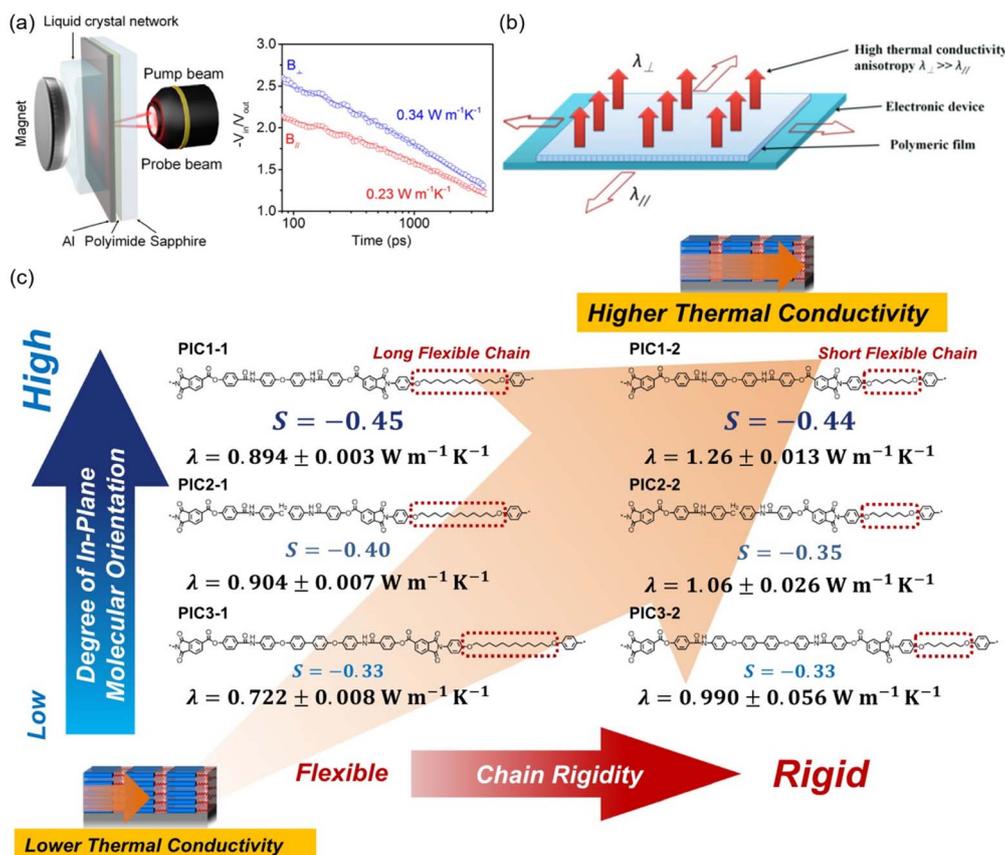This journal is © The Royal Society of Chemistry 2026

Fig. 7 Anisotropic thermal transport in LCN films. (a) Thermal conductivity measurements and TDTR fitting for films polymerized under parallel and perpendicular magnetic fields. Reproduced with permission.[217] Copyright 2016, American Chemical Society. (b) Schematic of anisotropic thermally conductive polymer films. Reproduced with permission.[220] Copyright 2017, Royal Society of Chemistry. (c) Correlation between chain rigidity, in-plane orientation, and thermal conductivity (λ). Reproduced with permission.[221] Copyright 2025, Springer Nature.
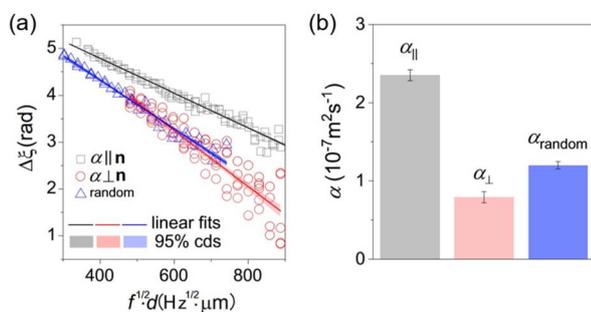

Fig. 8 Frequency-dependent thermal diffusivity in LCE films. (a) Phase delay $\Delta\xi$ of thermal waves propagating through LCE films of thickness d plotted as a function of the product $f^{1/2}d$, where f is the frequency of the heat source. Gray and red symbols correspond to thermal diffusivity α measured along and perpendicular to the director n in monodomain LCE films, respectively, while blue symbols represent α_{random} for polydomain LCE films. The phase delay decreases linearly with $f^{1/2}d$. (b) Thermal diffusivity values α extracted from the slopes of the linear fits in (a). Reproduced with permission.[229] Copyright 2022, Springer Nature.

or mechanical actuation, enabling passive yet adaptive thermal regulation without the need for electronics or external stimuli.

For example, Xiao et al. developed a Diels–Alder LCE doped with carbon nanotubes, engineered to undergo rapid deformation near 30 °C.[231] The material achieves an ultrahigh strain rate of 480%/s and exhibits self-sustained rolling motion under mild heating from body temperature or sunlight, demonstrating autonomous kinetic behavior suitable for wearable or soft robotic applications. Similarly, Vernerey et al. reported a helical-oriented LCE capable of over 2500% pre-programmed strain through a two-step synthesis.[232] With modest thermal inputs, this design supports large-scale, reversible deformation, emphasizing the versatility of LCEs for dynamic actuation in thermally responsive systems.

Ishii et al. incorporated LCE fibers into a textile system (FiberRoBra) designed to dynamically adjust its mechanical properties in response to body heat (Fig. 9(a)).[218] When worn, ambient thermal input triggers contraction of the aligned mesogens, increasing compressive support during periods of physical activity. As the body cools, the fibers relax, returning the textile to its original, less restrictive state. This reversible response requires no electronics, batteries, or sensors, allowing for a seamless, material-intrinsic form of intelligent wear regulated entirely by the user's body temperature.

Beyond actuation, LCEs also offer promising strategies for regulating fabric porosity through thermally driven shape

This journal is © The Royal Society of Chemistry 2026

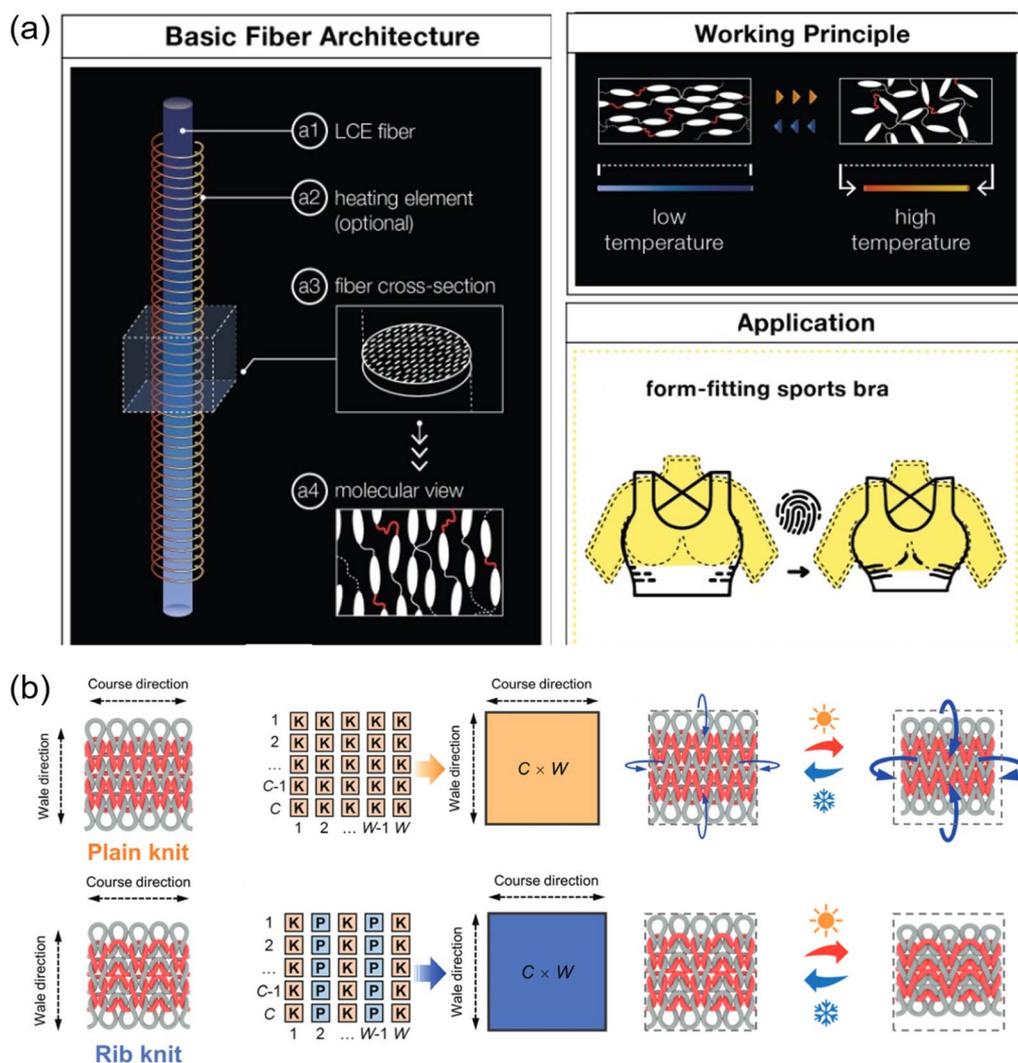J. Mater. Chem. A, 2026, 14, 3185–3209 | 3195

Fig. 9 LCE-based textile actuators. (a) Architecture and working principle of FibeRobo fibers and application in form-fitting sports bras. Reproduced with permission.[218] Copyright 2023, Association for Computing Machinery. (b) Thermal deformation of LCE actuators with knit and rib-knit patterns. Reproduced with permission.[233] Copyright 2023, John Wiley and Sons.

change.[234] Ahn *et al.* demonstrated that smectic-phase LCE fibers undergo axial elongation upon heating, achieving dynamic pore expansion perpendicular to the fiber direction when integrated as weft yarns in woven fabrics.[235] Building on this finding, Yang *et al.* incorporated LCE fibers into rib and plain stitch knitted structures (Fig. 9(b)).[233] Thermal contraction of the fibers generated torque that propagated through the textile network, producing saddle-shaped or helical 3D deformations. By adjusting stitch density and pattern, they achieved spatially controlled porosity modulation without requiring external power input.

More recently, Terentjev *et al.* demonstrated the compatibility of LCE yarns with conventional textile manufacturing techniques.[236] They successfully wove LCEs into standard architectures, including plain, satin, twill, and rib fabrics, each showing distinct thermally induced deformation behaviors. Among these, twill structures exhibited the greatest pore closure, attributed to their larger interlacing angles. In hybrid weaves combining LCEs with passive nylon or linen yarns, localized heating triggered reversible transformations from flat sheets to conical geometries, with porosity reductions exceeding 60% in targeted regions. These results demonstrate the potential of LCE yarns to act as embedded "smart hinges," illustrating their ability to provide precise, reversible control over ventilation and insulation in adaptive textile systems. Table 3 provides a concise comparison of LCE-based thermal management strategies, summarizing their material functions, performance metrics, key advantages, and current limitations.

4.4. Elastocaloric effect in LCEs for solid-state cooling

Elastocaloric effect refers to the reversible temperature change in a material upon mechanical stretching and contraction.[255,256] When a material is stretched or compressed, it may undergo an ordering transition, reducing its entropy and releasing heat (temperature increase). As shown in Fig. 10(a),[257] upon unloading, the material returns to a more disordered state,

3196 | *J. Mater. Chem. A*, 2026, **14**, 3185–3209

This journal is © The Royal Society of Chemistry 2026

Table 3 LCE-based thermal management strategies

Material functions	Performance	Key advantages of LCEs	Limitations and challenges	Ref.
Anisotropic thermal conductivity (4.1, 4.2)	Anisotropic thermal conductivity ratio: LCE $\lambda_\parallel/\lambda_\perp$ = 1–16 vs. traditional polymer 1–3 vs. nanofiller/polymer composite 1–100	Directional thermal management, tunable thermal conductivity, high-frequency compatibility	Limited long-term cycling stability; hard processing depending on the scale of materials	220, 237, 229, 238–242 and 243–246
	Axial thermal conductivity: LCE 0.22–1.44 W m^{-1} K^{-1} vs. traditional polymer 0.1–0.5 W m^{-1} K^{-1} vs. nanofiller/polymer composite 6–14 W m^{-1} K^{-1} vs. metal 200–400 W m^{-1} K^{-1} vs. carbon 1000–5000 W m^{-1} K^{-1}			73, 217, 219 and 247–251
Adaptive thermal insulation through mechanical deformation (4.3)	Porosity change: LCE fabric ~13% (wale) & ~18% (course) vs. composite fabric porosity increase of 38.3% from RT to 40 °C	Compatibility with weaving and knitting, passive responsiveness	Durability and high actuation temperature	232 and 252
	Response temperature: 25–120 °C			236, 253 and 254

absorbing heat from the surroundings and producing a cooling effect. This behavior follows classical thermodynamic relations, with key descriptors including the isothermal entropy change (ΔS) and adiabatic temperature change (ΔT). For polymers, these relationships are governed by the Maxwell relation:

$$\left(\frac{\partial S}{\partial \sigma}\right)_T = \left(\frac{\partial \varepsilon}{\partial T}\right)_\sigma \tag{1}$$

and the adiabatic response:

$$\Delta T_{ad} = -\frac{T}{C_p} \int_{\sigma_1}^{\sigma_2} \left(\frac{\partial \varepsilon}{\partial T}\right)_\sigma d\sigma \tag{2}$$

where ε is strain, σ is applied stress, T is temperature, and C_p is heat capacity at constant pressure. LCEs have recently surfaced as a promising elastocaloric material class due to their unique LC mesogen structures, which undergo stress-induced ordering transitions at relatively low stress levels. Unlike conventional elastocaloric materials such as shape-memory alloys[258] or natural rubber[259] which require large stress or strain to generate meaningful temperature changes, LCEs can trigger phase transitions and thus heat flow under moderate mechanical input.[260]

Several theoretical and experimental studies have demonstrated this potential. Skačej et al. employed large-scale molecular simulations using the Gay–Berne potential to predict the elastocaloric response of main-chain LCEs (Fig. 10(b)).[261] Their model estimated a temperature rise exceeding 10 K under 100 kPa of stress, suggesting a high responsivity (>100 K MPa^{-1}), although this value likely overestimates real performance. More refined Monte Carlo simulations by Kutnjak et al. investigated how crosslinker density influences the elastocaloric effect (Fig. 10(c)).[216] Their results showed that reducing crosslink density sharpens the phase transition and enhances responsivity, with simulated ΔT values up to 1.6 K at very low stress ($\Delta s = 0.056$ MPa; $\Delta T/\Delta s = 28$ K MPa^{-1}), corresponding to a realistic responsivity of ~28 K MPa^{-1}.

These findings were validated experimentally, showing comparable values (24.2 K MPa^{-1}).

On the experimental front, White et al. developed isotropic LCEs (IsoLCEs) with subambient transition temperatures and low hysteresis using a two-step thiol–ene crosslinking strategy.[257] These materials exhibit reversible temperature changes exceeding ±3 °C under low mechanical stress (<1 MPa), resulting in a total ΔT of 6 °C and a responsivity of ~14 °C MPa^{-1}, over seven times higher than natural rubber. As shown in Fig. 10(d),[257] these effects arise from deformation-induced alignment of mesogens and relaxation back to the isotropic state, permitting practical cooling cycles.

4.5. Challenges and opportunities

LCEs uniquely combine anisotropic thermal conductivity with programmable, stimuli-responsive deformation, enabling dynamic heat dissipation, thermal energy harvesting, adaptive insulation, and mechanically driven elastocaloric cooling. By coupling thermal regulation with mechanical actuation in lightweight, flexible architectures, they shift thermal management from passive control to actively reconfigurable behavior, positioning LCEs as promising materials for wearable electronics, soft robots, and high-frequency devices. As systems capable of autonomously adapting to changing environmental conditions, they provide a foundational platform for intelligent thermal management.

Despite this potential, translating LCEs from laboratory demonstrations to practical technologies requires overcoming several key challenges. A central scientific challenge is to decouple and independently optimize two critical parameters: the thermal anisotropy ratio and the absolute thermal conductivity. Achieving this goal will demand advanced molecular design strategies, combined with the controlled incorporation of anisotropically aligned fillers to enhance phonon transport within the polymer network without degrading the material's actuation response. At
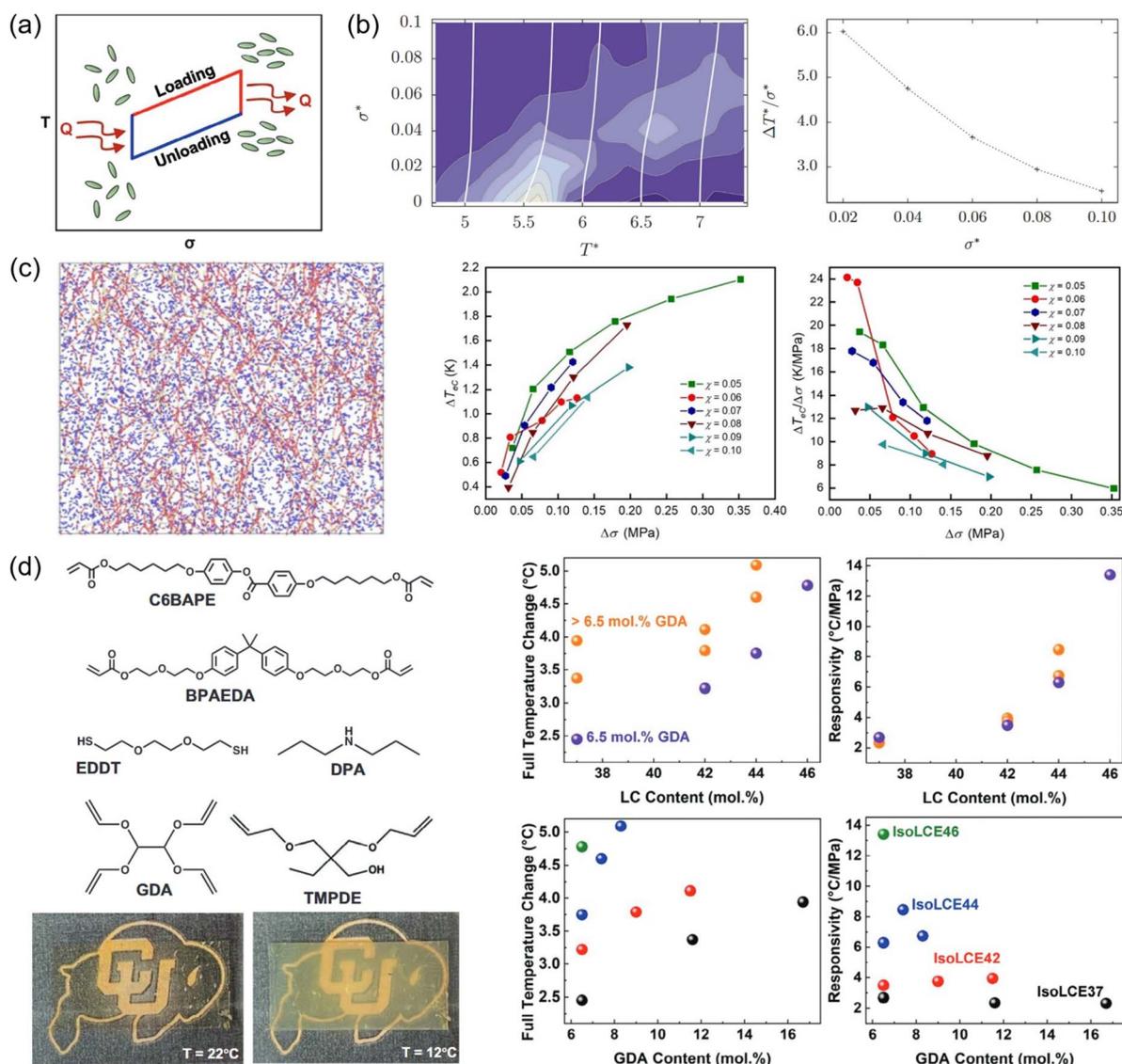
This journal is © The Royal Society of Chemistry 2026

J. Mater. Chem. A, 2026, **14**, 3185–3209 | **3197**

Fig. 10 Elastocaloric effect in LCEs: theoretical, computational, and experimental studies. (a) Elastocaloric cycle with temperature variation under loading and unloading. Reproduced with permission.[257] Copyright 2024, Johns Wiley and Sons. (b) Adiabatic curves and eC responsivity *versus* stress for $T^* = 5.5$ (below nematic–isotropic transition temperature). Reproduced with permission.[257] Copyright 2018, Taylor & Francis. (c) Simulated network topology after negative pressure shock (red: polymer strands; yellow: crosslinks; blue: swelling monomers) and ΔT_{eC} *versus* stress change (Δs) for varying crosslinker content. Reproduced with permission.[200] Copyright 2023, IOP Publishing. (d) Monomer structures, optical images above/below nematic–isotropic transition temperature, and measured ΔT and responsivity *versus* LC or crosslinker content. Reproduced with permission.[253] Copyright 2024, Johns Wiley and Sons.

the system level, a major obstacle lies in converting molecular-scale alignment into reliable macroscopic performance, particularly in smart textiles. This necessitates precise coordination between fiber spinning and fabric assembly to preserve orientation across hierarchical length scales and maintain continuous thermal pathways.

5. LCE in energy storage and electrochemical systems

Energy storage and electrochemical systems are technologies that capture, store and release energy through chemical reactions or electrical charge accumulation. Common examples include lithium-ion batteries,[262–264] supercapacitors,[265,266] and solid-state electrolytes.[267,268] These technologies are foundational to modern energy infrastructures, powering everything from portable electronics and electric vehicles to renewable energy systems. Recent advances in materials science have focused on improving energy density, flexibility, safety and integration into wearable or deformable devices.[269–271] In this context, LCEs offer exciting potential due to their unique combination of mechanical elasticity and anisotropic molecular ordering. Beyond conventional polymer electrolytes, LCEs have also been explored as mechanically adaptive components in lithium-ion and solid-state batteries, where their aligned mesogenic domains may facilitate directional ion transport and

3198 | *J. Mater. Chem. A*, 2026, **14**, 3185–3209

This journal is © The Royal Society of Chemistry 2026

Table 4 Comparison of LCE-based energy storage and electrochemical systems with conventional materials

Material system	Capacitance/ conductivity	Mechanical strain	Key advantages	Limitations and challenges	Ref.
LCE-based	40–120 F g^{-1}; 10^{-5}–10^{-3} S cm^{-1}	100–300%	Reversible shape morphing, programmable capacitance, anisotropic ion transport	Limited long-term cycling stability; incomplete understanding of alignment–ion coupling	70 and 272–274
Conductive polymer	100–500 F g^{-1}	<50%	High capacitance, facile processing	Mechanical fatigue, poor stretchability	275 and 276
Carbon-based	50–300 F g^{-1}	<10%	High conductivity, stable cycling	Rigid, low conformability	277 and 278
Gel/polymer electrolyte	10^{-4}–10^{-2} S cm^{-1}	50–200%	Flexible, safe	Limited strength, drying instability	279 and 280

deformation–tolerant interfaces. LCEs can be engineered to serve as flexible supercapacitors, solid-state electrolytes, or stretchable energy storage devices. Their stimuli-responsive shape deformability also opens new possibilities for self-adaptive, shape-morphing batteries and capacitors that operate reliably under strain or movement. Table 4 summarizes representative LCE-based energy storage and electrochemical systems, including flexible supercapacitors, solid-state electrolytes, and stretchable energy storage devices. The table outlines their key performance metrics and highlights how LCEs compare with conventional electrolytes and supercapacitors.

5.1. LCE-based flexible supercapacitors

LCEs could be employed as stretchable and adaptive platforms for electrochemical capacitors. Their ability to undergo large reversible deformations while maintaining conductivity allows for their use as structural and functional electrodes. Compared to traditional materials used in energy storage (*e.g.*, rigid carbon-based electrodes,[281] liquid electrolytes,[282] and polymer electrolytes[283]), LCE-based electrodes provide not only mechanical flexibility but also intrinsic shape-memory behavior, which enables adaptive performance under mechanical strain. While liquid electrolytes commonly used in lithium-ion batteries under risks of leakage and flammability, LCE-based solid electrolytes exhibit enhanced safety, flexibility, and integrated structural support. In contrast to static solid polymer electrolytes like polyethylene oxide (PEO)[284,285] and poly(vinylidene fluoride-hexafluoropropylene) (PVDF-HFP),[286,287] LCE systems can dynamically tune their mechanical and conductive properties through molecular alignment and phase transitions.

Ware *et al.* introduced an innovative platform for creating reconfigurable, 3D electronics using LCE substrates.[288] As shown in Fig. 11(a) and (b), the key design is the integration of functional passive components, including flexible capacitors, directly onto the shape-changing LCE substrate. The LCE-based capacitors are fabricated by embedding dielectric layers and patterned electrodes within or on top of the LCE sheet. As LCE deforms, the geometry of the capacitor (*e.g.*, area and thickness) changes, leading to a tunable capacitance. This property achieves not only reconfigurable circuits but also adaptive electronic behaviors such as variable filtering, sensing, or energy

storage capabilities without requiring rigid parts or external mechanical adjustment.

Recently, Feng *et al.* fabricated micro-supercapacitors by combining direct-ink-writing (DIW) 3D printing with electro-thermal LCEs as the structural substrate (Fig. 11(c–e)).[289] Electrodes and active materials are printed directly onto the LCE surface, forming integrated micro-supercapacitor arrays. The resulting devices are shape-programmable, capable of shape morphing through localized heating, while maintaining their energy storage functionality. The actuation of the LCE does not degrade the electrochemical performance, permitting conformal, reversible 3D transformation of energy storage devices in real time. Compared to conventional supercapacitors, these LCE-based platforms provide an unprecedented level of mechanical adaptability and programmability, making them ideal for future applications in soft robotics, adaptive electronics, and wearable systems.

5.2. LCE-based solid-state electrolytes

Solid-state electrolytes are materials that conduct ions while remaining in a solid phase, presenting a safer and more stable alternative to liquid electrolytes in batteries.[267,268] Furthermore, they offer improved thermal stability, non-flammability, and the ability to suppress short circuits in conventional batteries. LCEs offer a unique opportunity to enhance solid-state electrolytes due to their anisotropic molecular order and tunable mechanical properties. By incorporating ion-conductive species into the LCE matrix, researchers can develop materials that maintain ion transport capabilities while adapting mechanically to battery deformation or external stimuli.[70,272,290] This adaptability is particularly valuable in wearable or flexible electronics, where solid electrolytes must remain functional under repeated bending or stretching. Moreover, LCEs can provide a dynamic, phase-dependent balance between rigidity and flexibility, which can offer both structural support and ionic mobility depending on the operational conditions. In previous reported LCE–polymer composite electrolytes, ionic conductivities of 10^{-4}–10^{-3} S cm^{-1} have been achieved at room temperature, with lithium transference numbers exceeding 0.6 and stable cycling over 500 hours in Li–Li symmetric cells.[70,274] These results suggest that the mesogen orientation and microphase separation in LCE matrices can generate continuous ion-
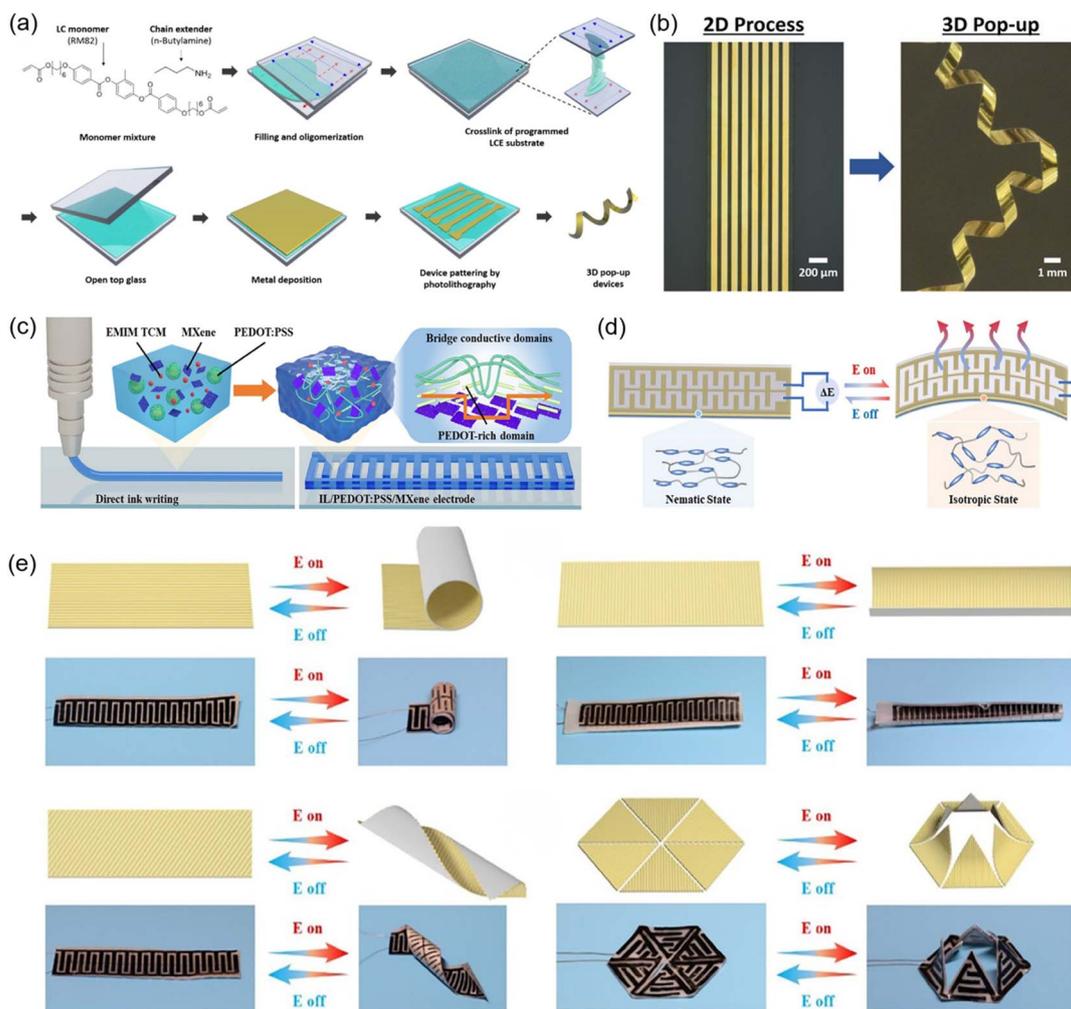
This journal is © The Royal Society of Chemistry 2026

J. Mater. Chem. A, 2026, **14**, 3185–3209 | **3199**

Fig. 11 Electrically actuated LCE-based programmable devices. (a) Molecular structures and fabrication steps.[288] (b) 3D pop-up LCE device. Reproduced with permission.[288] Copyright 2019, American Chemical Society. (c) Ionic liquid/poly(3,4-ethylenedioxythiophene):poly(styrene sulfonate) (PEDOT:PSS)/MXene inks with interdigital electrodes via DIW.[289] (d) Multilayer electrothermal LCE−micro-supercapacitor structure.[289] (e) Folding patterns of LCE−micro-supercapacitors with varied programmed shapes. Reproduced with permission.[188] Copyright 2025, John Wiley and Sons.

conduction channels, reducing polarization and suppressing dendrite growth.

Yang et al. reported a class of polymer electrolytes based on LCE networks that significantly enhance lithium-ion transport.[274] As shown in Fig. 12(a) and (b), the composite solid electrolyte, fabricated via UV-induced polymerization of LC monomers and poly(ethylene glycol) diglycidyl ether (PEGDE), forms a semi-interpenetrating network. This structure arises from self-assembly and microphase separation between the rigid mesogenic units and flexible polymer segments, producing continuous nano-ion transport channels. The resulting electrolytes exhibit enhanced ionic conductivity and high lithium ion transference number, attributed to a combination of amorphous poly(ethylene glycol) (PEG)-rich domains and ordered LCE regions that facilitate rapid ion migration. The system also maintains thermal stability, suppresses lithium dendrite growth, and enables long-term cycling in lithium metal batteries.

Miao et al. reported another advancement in LCE-based ion-conducting solid electrolytes.[70] As shown in Fig. 12(c), an LCE-based solid electrolyte exhibits tunable mechanical properties of shifting between rigid and flexible states, depending on operational demands to improve the performance and safety of high-energy lithium batteries. In the system, the LCE domains serve as dynamic structural frameworks that can reorganize under thermal or mechanical stimuli, allowing the material to become stiffer during charging and discharging cycles or more flexible to adapt to mechanical deformation in wearable devices. In addition, this design avoids the leakage and flammability risks associated with liquid electrolytes while supporting efficient lithium-ion transport across the membrane. Beyond lithium systems, emerging work has applied LCE frameworks to zinc- and sodium-based batteries, where the elastic networks accommodate large-volume changes and prevent interfacial cracking during cycling.[70,291] Overall, LCE-based solid-state electrolytes combine anisotropic ion
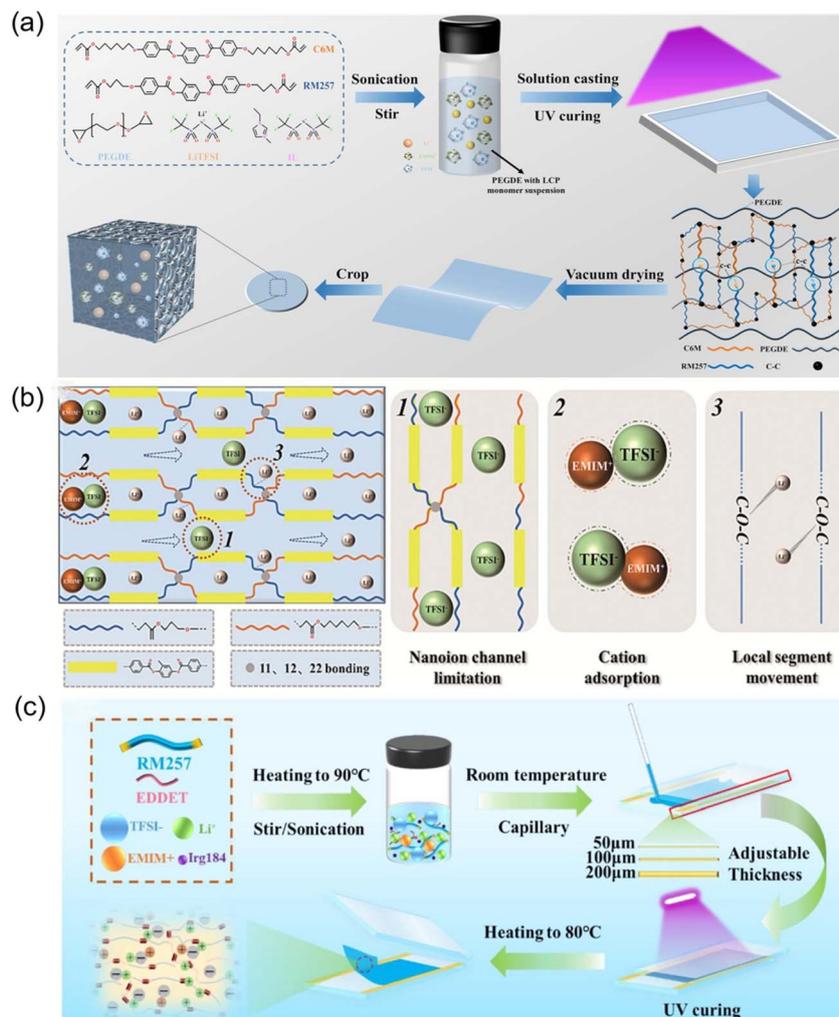
3200 | J. Mater. Chem. A, 2026, 14, 3185–3209

This journal is © The Royal Society of Chemistry 2026

Fig. 12 Fabrication and ion transport in LC polymer−ionic liquid composites. (a) Preparation of polymer composite electrolytes (PCREs).[270] (b) Schematic of rapid lithium ion transport mechanism in PCREs. Reproduced with permission.[270] Copyright 2023, Elsevier. (c) LCE−solid polymer electrolyte manufacturing route. Reproduced with permission.[70] Copyright 2025, Elsevier.

transport and mechanical adaptability, offering a promising solution for safe, flexible, and high-performance lithium metal batteries.

5.3. LCE-based stretchable and shape-morphing energy storage devices

Stretchable energy storage devices contain batteries, supercapacitors and hybrid systems that maintain reliable energy storage and delivery performance while being bent, stretched, or twisted.[292–294] These devices are essential for the development of wearable electronics,[18,269,270] soft robotics,[106,178] and biomedical implants,[19,295] where conventional rigid energy systems are unsuitable due to their lack of mechanical compliance. To function effectively in these dynamic environments, stretchable energy storage devices require soft materials that combine electrochemical performance with high mechanical deformability. LCEs offer a promising platform for these applications because of their inherent elasticity, programmable shape deformability, and molecular alignment. Furthermore, they can

be designed to serve as active substrates, electrodes, or even electrolyte matrices in stretchable power systems. The anisotropic mechanical behavior of LCEs, combined with their ability to respond to external stimuli, support unique functionalities like on-demand shape reconfiguration, strain-adaptive capacitance, or localized ion transport. These effects bridge energy conversion and storage, representing hybrid systems where deformation-driven electrical generation directly supports or recharges local energy reservoirs within the same LCE platform. These properties allow LCE-based devices to actively modulate performance based on deformation states, providing a new dimension of adaptability for energy storage technologies in dynamic environments.

Jákli *et al.* reported a novel coupling mechanism between mechanical deformation and ionic charge redistribution within ionic LCEs. These systems exhibit the flexo-ionic effect, where strain gradients induce directional ion migration, generating a measurable voltage across the material (Fig. 13(a)).[272] This mechano-electrochemical interaction allows LCEs to operate as both actuators and soft energy harvesters. The study

This journal is © The Royal Society of Chemistry 2026

J. Mater. Chem. A, 2026, **14**, 3185–3209 | **3201**

demonstrates that bending the elastomer modulates internal ionic distribution, leading to voltage generation without external circuitry. Compared to traditional piezoelectric materials, ionic LCEs provide greater stretchability, enhanced conformability, and tunable sensitivity *via* molecular alignment, with potential use in wearable sensors, soft robotics, and integrated power systems in stretchable electronics.

Furthermore, Majidi *et al.* reported an LCE system that couples mechanical deformation with thermoelectric conversion, allowing both energy storage and harvesting.[183] The LCE serves as a soft, deformable scaffold with anisotropic alignment that achieves programmable shape-memory behavior. When combined with thermoelectric nanomaterials, such as Bi_2Te_3 particles, the composite material not only deforms under heat but also generates electrical output due to the resulting thermal gradients, as shown in Fig. 13(b) and (c). These results demonstrate the potential of LCEs to serve as active components in stretchable and shape-morphing energy storage devices. Coupling such deformation-driven charge redistribution with embedded electrochemical electrodes could achieve hybrid systems where LCEs simultaneously function as mechanical actuators and local energy reservoirs, bridging the gap between energy harvesting and storage. By using LCE elasticity, molecular alignment, and stimulus-responsiveness, these systems permit both energy delivery and harvesting, with potential applications for wearable and soft electronics.

5.4. Challenges and opportunities

LCE-based energy storage systems offer significant promise as multifunctional materials that combine mechanical adaptability with electrochemical performance. However, several key challenges remain before these systems can achieve practical implementation.

A major challenge is the limited understanding of the relationship between molecular alignment and ion transport within anisotropic LCE matrices. Ionic mobility depends strongly on mesogen orientation, crosslink density, and the morphology of phase-separated ion-conductive domains. Quantitative insight into how molecular order governs ion migration along and across the director remains limited. More systematic studies combining *in situ* characterization with modeling are needed to clarify how ion motion couples with deformation and phase transitions in LCE networks.

Another important issue is the coupling between mechanical deformation and electrochemical behavior. Repeated deformation can disrupt ion transport pathways or change local concentration distributions, leading to performance loss. Designing crosslinking structures that maintain conductivity under cyclic strain, such as dual-network or dynamic bond systems, will be key to improving reliability.

Long-term durability is also a concern. Repeated actuation and environmental exposure can cause mechanical fatigue or chemical degradation of mesogens and ionic components. Strategies including the use of UV-stable mesogens, oxidation-resistant ionic liquids, and optimized encapsulation are essential to ensure durability under continuous operation.

Processing scalability remains a major challenge. Current alignment methods such as surface rubbing or photoalignment are limited to small areas. Field-assisted alignment, additive manufacturing, and self-templating polymerization offer more viable routes toward uniform, large-scale, defect-free LCE structures suitable for device integration.

Finally, integrating LCEs into multifunctional energy systems that couple mechanical adaptability, ion transport, and sensing functions within a single platform offers a promising direction. Such integration could permit the design of self-
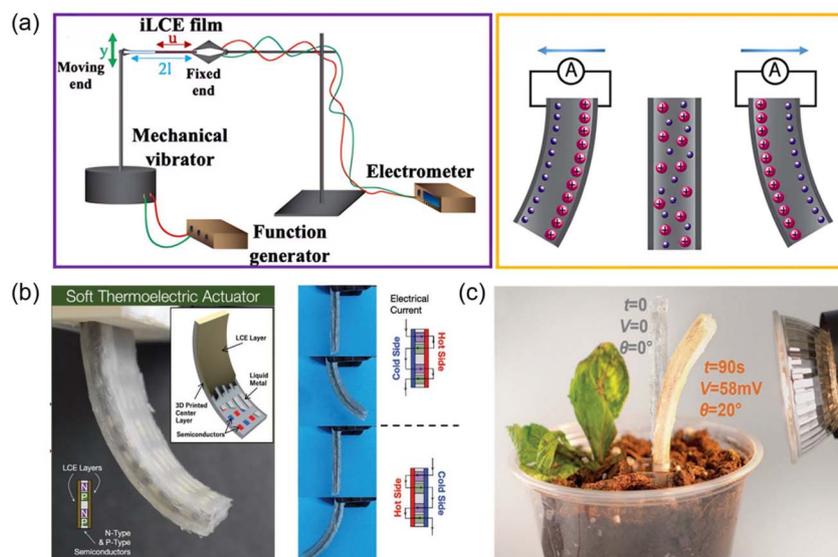
Fig. 13 Energy harvesting and actuation in ionic and thermoelectric LCE systems. (a) Experimental circuit and mechanism of the flexo-ionic effect. Reproduced with permission.[272] Copyright 2021, MDPI. (b) Actuator with LCE layer, embedded semiconductors, and liquid metal interconnects on 3D-printed substrate.[183] (c) Autonomous bending toward a heat source with simultaneous voltage generation. Reproduced with permission.[183] Copyright 2022, John Wiley and Sons.

healing supercapacitors, deformable solid-state batteries, and hybrid systems capable of energy harvesting and storage. The intrinsic anisotropy and stimulus-responsiveness of LCEs provide a foundation for developing adaptive energy materials that can dynamically regulate electrochemical and mechanical response in real time.

6. Conclusion

LCEs offer a compelling platform for next-generation energy technologies due to their combination of molecular order, mechanical flexibility, and stimuli-responsive behavior. Across solar, electronic, thermal, and electrochemical systems, LCEs exhibit dynamic functions such as autonomous actuation, directional conductivity, adaptive thermal insulation, and shape-responsive energy storage. Furthermore, LCEs play a central role in the development of intelligent energy systems that can sense, adapt, and respond to their environment. By bridging soft materials science with practical device engineering, future research in LCEs may unlock a new generation of energy devices that are flexible, efficient, and autonomously reconfigurable.

Despite the broad promise, several technical challenges remain. These challenges include improving energy conversion efficiency, maintaining molecular alignment and structural stability during operation, and scaling fabrication methods suitable for device integration. For solar energy harvesting systems, limited light-responsive wavelength, scalable fabrication and long-term durability are still main challenges. Molecular optimization, for instance, expanding π-conjugation in azobenzene structure or incorporating donor–acceptor substituents, offers one promising strategy to broaden adsorption wavelength. Developing processable LCEs inks for 3D printing has provided insights for large-scale fabrication. Additionally, dynamic covalent chemistry is one potential way to improve photochemical fatigue resistance, contributed by the energy dissipation mechanism and self-repair ability in dynamic polymer network. For electrochemical and energy-storage systems, the main challenges lie in understanding how mesogen alignment governs ion transport, improving ionic conductivity while maintaining elasticity, and designing crosslinking networks that remain stable under repeated deformation. Progress also requires scalable alignment and fabrication methods, such as field-assisted polymerization or direct-ink-writing of anisotropic domains, to build large-area, defect-free devices. Developing these approaches will be key to translating LCE-based solid-state electrolytes and supercapacitors into practical soft-energy systems.

Although light, heat, and chemical stimuli remain the dominant activation modes for LCEs, electrical actuation is more limited. Most dielectric LCE actuators require kilovolt-level fields to generate meaningful strains, far higher than the sub-5 V operation typical of conducting polymers or ionic electroactive systems.[296–300] In many reported devices, the apparent "electrical actuation" arises primarily from Joule heating or thermoelectric coupling rather than direct field-induced reorientation of mesogens.[15,183,301–303] These constraints, combined with modest electromechanical efficiency, have so far restricted electrically driven LCEs from practical low-voltage applications. Nevertheless, reducing operating voltage through enhanced dielectric permittivity, composite design, and nanoscale alignment control represents an important opportunity for future research, and remains one of the most promising directions for expanding the functional scope of LCE-based energy systems.

Author contributions

MZ, XL, TY, and HH contributed equally to the conception, literature review, and drafting of the manuscript. YY, SL and XW supervised the work, coordinated the overall project, and contributed to the manuscript drafting. All authors have read and revised the manuscript.

Conflicts of interest

There are no conflicts to declare.

Data availability

No primary research results, software or code have been included and no new data were generated or analysed as part of this review.

Acknowledgements

References

1 J. Prost and P. S. Pershan, *J. Appl. Phys.*, 1976, **47**, 2298–2312.

2 P.-G. de Gennes and J. Prost, *The Physics of Liquid Crystals*, Oxford University Press, 1993.

3 E. Bukusoglu, M. Bedolla Pantoja, P. C. Mushenheim, X. Wang and N. L. Abbott, *Annu. Rev. Chem. Biomol. Eng.*, 2016, **7**, 163–196.

4 I. Dierking, *Symmetry*, 2014, **6**, 444–472.

5 Y. Zhou, E. Bukusoglu, J. A. Martínez-González, M. Rahimi, T. F. Roberts, R. Zhang, X. Wang, N. L. Abbott and J. J. de Pablo, *ACS Nano*, 2016, **10**, 6484–6490.

6 J. J. de Pablo, Q. Yan and F. A. Escobedo, *Annu. Rev. Phys. Chem.*, 1999, **50**, 377–411.

7 E. M. Terentjev, *Macromolecules*, 2025, **58**, 2792–2806.

8 T. J. White and D. J. Broer, *Nat. Mater.*, 2015, **14**, 1087–1098.

9 D. Chen, J. H. Porada, J. B. Hooper, A. Klittnick, Y. Shen, M. R. Tuchband, E. Korblova, D. Bedrov, D. M. Walba, M. A. Glaser, M. A. Glaser, J. E. Maclennan and N. A. Clark, *Proc. Natl. Acad. Sci. U. S. A.*, 2013, **110**, 15931–15936.

10 X. Wang, D. S. Miller, E. Bukusoglu, J. J. de Pablo and N. L. Abbott, *Nat. Mater.*, 2016, **15**, 106–112.

This journal is © The Royal Society of Chemistry 2026

J. Mater. Chem. A, 2026, **14**, 3185–3209 | **3203**

11 X. Wang, Y.-K. Kim, E. Bukusoglu, B. Zhang, D. S. Miller and N. L. Abbott, *Phys. Rev. Lett.*, 2016, **116**, 147801.

12 J. Küpfer and H. Finkelmann, *Makromol. Chem., Rapid Commun.*, 1991, **12**, 717–726.

13 R. Mouhoubi, V. Lapinte and S. Blanquer, *Adv. Funct. Mater.*, 2025, **26**, 2424400.

14 Y. Sun, L. Wang, Z. Zhu, X. Li, H. Sun, Y. Zhao, C. Peng, J. Liu, S. Zhang and M. Li, *Adv. Mater.*, 2023, **35**, 2302824.

15 H. E. Fowler, P. Rothemund, C. Keplinger and T. J. White, *Adv. Mater.*, 2021, **33**, 2103806.

16 J. Ma and Z. Yang, *Matter*, 2025, **8**, 101950.

17 W. Ji, B.-y. Wei, P. Chen, W. Hu and Y.-q. Lu, *Mol. Cryst. Liq. Cryst.*, 2017, **644**, 3–11.

18 Z. Huang, L. Li, T. Wu, T. Xue, W. Sun, Q. Pan, H. Wang, H. Xie, J. Chi, T. Han, X. Hu, M. Su, Y. Chen and Y. Song, *Nat. Commun.*, 2023, **14**, 1204.

19 M. Prévôt, H. Andro, S. Alexander, S. Ustunel, C. Zhu, Z. Nikolov, S. Rafferty, M. Brannum, B. Kinsel, L. Korley, E. Freeman, J. McDonough, R. Clements and E. Hegmann, *Soft Matter*, 2018, **14**, 354–360.

20 R. L. Dupont, Y. Xu, A. Borbora, X. Wang, F. Azadi, K. Havener, B. Lewis, W. Deng, B. W. Tan, S. Li, R. Zhang, Y. Yao, U. Manna and X. Wang, *Adv. Mater.*, 2025, **37**, 2414695.

21 X. Wang, D. S. Miller, J. J. de Pablo and N. L. Abbott, *Adv. Funct. Mater.*, 2014, **24**, 6219–6226.

22 H. Xing, J. Li, Y. Shi, J. Guo and J. Wei, *ACS Appl. Mater. Interfaces*, 2016, **8**, 9440–9445.

23 H. Xing, J. Li, Y. Shi, J. Guo and J. Wei, *ACS Appl. Mater. Interfaces*, 2016, **8**, 9440–9445.

24 R. Annapooranan and S. Cai, *Eng. Fract. Mech.*, 2022, **269**, 108584.

25 V. Maurin, Y. Chang, Q. Ze, S. Leanza, J. Wang and R. R. Zhao, *Adv. Mater.*, 2024, **36**, 2302765.

26 Y. Xu, R. L. Dupont, Y. Yao, M. Zhang, J.-C. Fang and X. Wang, *Macromolecules*, 2021, **54**, 5376–5387.

27 Y. Yao, A. M. Wilborn, B. Lemaire, F. Trigka, F. Stricker, A. H. Weible, S. Li, R. K. Bennett, T. C. Cheung, A. Grinthal, M. Zhernenkov, G. Freychet, P. Wąsik, B. Kozinsky, M. M. Lerch, X. Wang and J. Aizenberg, *Science*, 2024, **386**, 1161–1168.

28 M. Barnes and R. Verduzco, *Soft Matter*, 2019, **15**, 870–879.

29 A. Agrawal, T. Yun, S. L. Pesek, W. G. Chapman and R. Verduzco, *Soft Matter*, 2014, **10**, 1411–1415.

30 Y.-K. Kim, X. Wang, P. Mondkar, E. Bukusoglu and N. L. Abbott, *Nature*, 2018, **557**, 539–544.

31 Z. Pei, Y. Yang, Q. Chen, E. M. Terentjev, Y. Wei and Y. Ji, *Nat. Mater.*, 2014, **13**, 36–41.

32 W. Feng, D. Liu and D. J. Broer, *Small Struct.*, 2021, **2**, 2000107.

33 Z. Wu, W. Zhang, W. Xu, Q. Chen, M. Liu, Y. Liu, Q. Zhang, W. Hu, D. Liu, Y. Q. Lu and D. Luo, *Adv. Funct. Mater.*, 2025, e13461.

34 Y. Li, Y. Liu and D. Luo, *Adv. Opt. Mater.*, 2021, **9**, 2001861.

35 H. Tian, Z. Wang, Y. Chen, J. Shao, T. Gao and S. Cai, *ACS Appl. Mater. Interfaces*, 2018, **10**, 8307–8316.

36 L. H. Mahajan, D. Ndaya, P. Deshmukh, X. Peng, M. Gopinadhan, C. O. Osuji and R. M. Kasi, *Macromolecules*, 2017, **50**, 5929–5939.

37 Y. Song, J. Zhang, Z. Sun, H. Liang, T. Sun, Z. Lu, S. Li, Y. Yao, X. Wang, Y. Xu and J. Huang, *InfoMat*, 2025, **7**, e70008.

38 C. L. Van Oosten, C. W. Bastiaansen and D. J. Broer, *Nat. Mater.*, 2009, **8**, 677–682.

39 A. H. Gelebart, D. Jan Mulder, M. Varga, A. Konya, G. Vantomme, E. Meijer, R. L. Selinger and D. J. Broer, *Nature*, 2017, **546**, 632–636.

40 Z. Deng, K. Li, A. Priimagi and H. Zeng, *Nat. Mater.*, 2024, **23**, 1728–1735.

41 P. Shi, Y. Zhao, Z. Liu and X. He, *J. Compos. Mater.*, 2023, **57**, 633–643.

42 P. Hogan, A. Tajbakhsh and E. Terentjev, *Phys. Rev. E*, 2002, **65**, 041720.

43 H. Zeng, O. M. Wani, P. Wasylczyk, R. Kaczmarek and A. Priimagi, *Adv. Mater.*, 2017, **29**, 1701814.

44 Y. Sun, J. S. Evans, T. Lee, B. Senyuk, P. Keller, S. He and I. Smalyukh, *Appl. Phys. Lett.*, 2012, **100**, 241901.

45 J. Zhang, Y. Guo, W. Hu, R. H. Soon, Z. S. Davidson and M. Sitti, *Adv. Mater.*, 2021, **33**, 2006191.

46 J. M. Boothby, H. Kim and T. H. Ware, *Sens. Actuators, B*, 2017, **240**, 511–518.

47 R. Lan, W. Shen, W. Yao, J. Chen, X. Chen and H. Yang, *Mater. Horiz.*, 2023, **10**, 2824–2844.

48 S. Jing, J. Huang, H. Wang, Y. Wang, H. Xie and S. Zhou, *ACS Appl. Mater. Interfaces*, 2024, **16**, 25404–25414.

49 M. O. Astam, P. Lyu, J. Peixoto and D. Liu, *Soft Matter*, 2022, **18**, 7236–7244.

50 Y. Liu, Y. Wu, H. Liang, H. Xu, Y. Wei and Y. Ji, *Adv. Funct. Mater.*, 2023, **33**, 2302110.

51 V. Percec and A. Keller, *Macromolecules*, 1990, **23**, 4347–4350.

52 B. Donnio, H. Wermter and H. Finkelmann, *Macromolecules*, 2000, **33**, 7724–7729.

53 A. Sánchez-Ferrer, T. Fischl, M. Stubenrauch, H. Wurmus, M. Hoffmann and H. Finkelmann, *Macromol. Chem. Phys.*, 2009, **210**, 1671–1677.

54 H. Finkelmann and G. Rehage, *Makromol. Chem. Rapid Commun.*, 1980, **1**, 31–34.

55 J. Kupfer and H. Finkelman, *Makromol. Chem. Rapid Commun.*, 1991, **12**, 717.

56 R. Zentel, G. F. Schmidt, J. Meyer and M. Benalia, *Liq. Cryst.*, 1987, **2**, 651.

57 P. Beyer, L. Braun and R. Zentel, *Macromol. Chem. Phys.*, 2007, **208**, 2439.

58 T. Padmavathy and K. Srinivasan, *J. Macromol. Sci., Part C: Polym. Rev.*, 2003, **43**, 45–85.

59 S. J. Sun, K. Y. Hsu and T. C. Chang, *J. Polym. Sci., Part A: Polym. Chem.*, 1995, **33**, 787–796.

60 J. Naciri, A. Srinivasan, H. Jeon, N. Nikolov, P. Keller and B. R. Ratna, *Macromolecules*, 2003, **36**, 8499–8505.

61 H. Yang, Y. J. Lv, B. P. Lin, X. Q. Zhang, Y. Sun and L. X. Guo, *J. Polym. Sci., Part A: Polym. Chem.*, 2014, **52**, 1086–1098.

3204 | *J. Mater. Chem. A*, 2026, **14**, 3185–3209

This journal is © The Royal Society of Chemistry 2026

62 Y. Xia, R. Verduzco, R. H. Grubbs and J. A. Kornfield, *J. Am. Chem. Soc.*, 2008, **130**, 1735–1740.

63 E.-K. Fleischmann, F. R. Forst, K. Köder, N. Kapernaum and R. Zentel, *J. Mater. Chem. C*, 2013, **1**, 5885–5891.

64 T. H. Ware, Z. P. Perry, C. M. Middleton, S. T. Iacono and T. J. White, *ACS Macro Lett.*, 2015, **4**, 942–946.

65 L. Wang, W. Liu, L.-X. Guo, B.-P. Lin, X.-Q. Zhang, Y. Sun and H. Yang, *Polym. Chem.*, 2017, **8**, 1364–1370.

66 P. Beyer, L. Braun and R. Zentel, *Macromol. Chem. Phys.*, 2007, **208**, 2439–2448.

67 M. H. Li, P. Keller, J. Y. Yang and P. A. Albouy, *Adv. Mater.*, 2004, **16**, 1922.

68 M. Brehmer, R. Zentel, G. Wagenblast and K. Siemensmeyer, *Macromol. Chem. Phys.*, 1994, **195**, 1891.

69 E. Gebhard and R. Zentel, *Macromol. Rapid Commun.*, 1998, **19**, 341.

70 X. Wang, Z. He, R. Yan, H. Niu, W. He and Z. Miao, *Chem. Eng. J.*, 2025, **503**, 158552.

71 S. Y. Jeon, B. Shen, N. A. Traugutt, Z. Zhu, L. Fang, C. M. Yakacki, T. D. Nguyen and S. H. Kang, *Adv. Mater.*, 2022, **34**, 2200272.

72 L. Li, X. Dong, J. Xu, Y. Jiang, X. Zhou, Q. Li, N. Yuan and J. Ding, *Sens. Actuators, B*, 2023, **390**, 133846.

73 Y. Ma, J. You, L. Zhang, R. Chen, H. Zeng, J. Ge, K. Li, X. Ma, A. K. Y. Jen and S. Liu, *Adv. Funct. Mater.*, 2024, **34**, 2405250.

74 C. Li, Y. Liu, X. Huang and H. Jiang, *Adv. Funct. Mater.*, 2012, **22**, 5166–5174.

75 Y. Ding, Y. Bai, T. Wang, Z. Gao, Y. Gao, X. Wang, B. Li, P. Wang, C. Dai, X. Wang and Z. Li, *Polym. Compos.*, 2025, 1–12.

76 X. Lu, S. Guo, X. Tong, H. Xia and Y. Zhao, *Adv. Mater.*, 2017, **29**, 1606467.

77 Z. Ju, X. Tao, Y. Wang, Q. Yang, T. Liu, J. Nai, W. Zhang, S. Chen, Y. Liu and H. Tian, *Energy Environ. Sci.*, 2024, **17**, 4703–4713.

78 W. Wei, J. Gao, J. Yang, J. Wei and J. Guo, *RSC Adv.*, 2018, **8**, 40856–40865.

79 Y. Zhou and G. Li, *Photonics*, 2025, **12**, 819.

80 H. Sentjens, A. J. J. Kragt, A. P. H. J. Schenning and M. G. Debije, *Responsive Mater.*, 2023, **1**, e20230006.

81 X. Meng, S. Lin, S. Chen, X. Shen, D. Guo and J. Guo, *ChemPlusChem*, 2024, **89**, e202300700.

82 F. Zhai, Y. Feng, K. Zhou, L. Wang, Z. Zheng and W. Feng, *J. Mater. Chem. C*, 2019, **7**, 2146–2171.

83 M. Yang, Y. Xu, X. Zhang, H. K. Bisoyi, P. Xue, Y. Yang, X. Yang, C. Valenzuela, Y. Chen and L. Wang, *Adv. Funct. Mater.*, 2022, **32**, 2201884.

84 F. Wang, R. Bi, Y. Chen, Y. Yang, Y. Liu, L. Yang, Y. Shen, L. Wang and W. Feng, *Mater. Horiz.*, 2025, **12**, 5315–5324.

85 S. Yang, S. Tang, X. Yuan, X. Zou, H. Zeng, Y. Song, M. X. Hu, M. Liu and B. Li, *Adv. Funct. Mater.*, 2025, e11552.

86 M. Chen, H. Huang, Y. Zhu, Z. Liu, X. Xing, F. Cheng and Y. Yu, *Appl. Phys. A*, 2011, **102**, 667–672.

87 Y. Huang, Q. Yu, C. Su, J. Jiang, N. Chen and H. Shao, *Actuators*, 2021, **10**, 298.

88 X. Pang, J. a. Lv, C. Zhu, L. Qin and Y. Yu, *Adv. Mater.*, 2019, **31**, 1904224.

89 L. Hernández-Callejo, S. Gallardo-Saavedra and V. Alonso-Gómez, *Sol. Energy*, 2019, **188**, 426–440.

90 P. G. V. Sampaio and M. O. A. González, *Renewable Sustainable Energy Rev.*, 2017, **74**, 590–601.

91 J. Siecker, K. Kusakana and e. B. Numbi, *Renewable Sustainable Energy Rev.*, 2017, **79**, 192–203.

92 S. A. Kalogirou, *Prog. Energy Combust. Sci.*, 2004, **30**, 231–295.

93 L. Evangelisti, R. D. L. Vollaro and F. Asdrubali, *Renewable Sustainable Energy Rev.*, 2019, **114**, 109318.

94 H. Guo, M. O. Saed and E. M. Terentjev, *Adv. Mater. Technol.*, 2021, **6**, 2100681.

95 X. Qian, Y. Zhao, Y. Alsaid, X. Wang, M. Hua, T. Galy, H. Gopalakrishna, Y. Yang, J. Cui and N. Liu, *Nat. Nanotechnol.*, 2019, **14**, 1048–1055.

96 S.-Y. Jung, S. Han, M.-G. Lee and H. Lee, *Buildings*, 2022, **12**, 2017.

97 B. Tylkowski, A. Trojanowska, V. Marturano, M. Nowak, L. Marciniak, M. Giamberini, V. Ambrogi and P. Cerruti, *Coord. Chem. Rev.*, 2017, **351**, 205–217.

98 Y. Yu, T. Maeda, J. i. Mamiya and T. Ikeda, *Angew. Chem., Int. Ed.*, 2007, **46**, 881–883.

99 L. Ceamanos, D. J. Mulder, Z. Kahveci, M. López-Valdeolivas, A. P. Schenning and C. Sánchez-Somolinos, *J. Mater. Chem. B*, 2023, **11**, 4083–4094.

100 K. J. Tangso, W.-K. Fong, T. Darwish, N. Kirby, B. J. Boyd and T. L. Hanley, *J. Phys. Chem. B*, 2013, **117**, 10203–10210.

101 G. Stoychev, A. Kirillova and L. Ionov, *Adv. Opt. Mater.*, 2019, **7**, 1900067.

102 M. M. Sroda, J. Lee, Y. Kwon, F. Stricker, M. Park, M. T. Valentine and J. Read de Alaniz, *ACS Appl. Polym. Mater.*, 2022, **4**, 141–149.

103 Z. Li, Z. Wang, X. Chen, J. Bao, Y. Zhang, Z. Wang, L. Zhang, J. Xiao, R. Lan and H. Yang, *Adv. Mater.*, 2024, **36**, 2411530.

104 G. Long, Y. Deng, W. Zhao, G. Zhou, D. J. Broer, B. L. Feringa and J. Chen, *J. Am. Chem. Soc.*, 2024, **146**, 13894–13902.

105 S. Xie, A. Natansohn and P. Rochon, *Chem. Mater.*, 1993, **5**, 403–411.

106 J. Ince, K. Prasad, K. Subhani, A. Duffy and N. Salim, *Adv. Compos. Hybrid Mater.*, 2024, **7**, 186.

107 J. Sun, Y. Wang, W. Liao and Z. Yang, *Small*, 2021, **17**, 2103700.

108 Y. Yu, L. Li, E. Liu, X. Han, J. Wang, Y.-X. Xie and C. Lu, *Carbon*, 2022, **187**, 97–107.

109 Y. Liu, J. Ma, Y. Yang, C. Valenzuela, X. Zhang, L. Wang and W. Feng, *Smart Mol.*, 2024, **2**, e20230025.

110 Y. Xu, A. M. Rather, Y. Yao, J.-C. Fang, R. S. Mamtani, R. K. Bennett, R. G. Atta, S. Adera, U. Tkalec and X. Wang, *Sci. Adv.*, 2021, **7**, eabi7607.

111 D. Liu and D. J. Broer, *Angew. Chem., Int. Ed.*, 2014, **53**, 4542–4546.

112 S. A. Weima, R. Norouzikudiani, J. Baek, J. A. Peixoto, T. K. Slot, D. J. Broer, A. DeSimone and D. Liu, *Sci. Adv.*, 2024, **10**, eadp0421.

113 J. Xu, S. Chen, W. Yang, B. Qin, X. Wang, Y. Wang, M. Cao, Y. Gao, C. Li and Y. Dong, *Soft Matter*, 2019, **15**, 6116–6126.

This journal is © The Royal Society of Chemistry 2026

J. Mater. Chem. A, 2026, **14**, 3185–3209 | **3205**

114 K.-W. Yeung, Y. Dong, L. Chen, C.-Y. Tang, W.-C. Law, G. C.-P. Tsui and D. S. Engstrøm, *Nanotechnol. Rev.*, 2020, **9**, 418–426.

115 Y.-S. Zhang, S.-A. Jiang, J.-D. Lin and C.-R. Lee, *J. Mater. Chem. C*, 2020, **8**, 5517–5524.

116 S. Mori, H. Takagi, N. Shimizu, N. Igarashi, S. Sakurai and K. Urayama, *Soft Matter*, 2024, **20**, 3931–3941.

117 S. S. Lee, J. B. Kim, Y. H. Kim and S.-H. Kim, *Sci. Adv.*, 2018, **4**, eaat8276.

118 H. Xing, J. Li, J. Guo and J. Wei, *J. Mater. Chem. C*, 2015, **3**, 4424–4430.

119 P. Zhang, L. T. de Haan, M. G. Debije and A. P. Schenning, *Light Sci. Appl.*, 2022, **11**, 248.

120 S. Woska, A. Münchinger, D. Beutel, E. Blasco, J. Hessenauer, O. Karayel, P. Rietz, S. Pfleging, R. Oberle, C. Rockstuhl, M. Wegener and H. Kalt, *Opt. Mater. Express*, 2020, **10**, 2928–2943.

121 S. Nocentini, D. Martella, C. Parmeggiani and D. S. Wiersma, *Materials*, 2016, **9**, 525.

122 X. Liang, S. Guo, M. Chen, C. Li, Q. Wang, C. Zou, C. Zhang, L. Zhang, S. Guo and H. Yang, *Mater. Horiz.*, 2017, **4**, 878–884.

123 X. Liang, M. Chen, S. Guo, L. Zhang, F. Li and H. Yang, *ACS Appl. Mater. Interfaces*, 2017, **9**, 40810–40819.

124 I. S. Osman and N. G. Hariri, *Sustainability*, 2022, **14**, 5078.

125 S. Y. Obara, K. Matsumura, S. Aizawa, H. Kobayashi, Y. Hamada and T. Suda, *Sol. Energy*, 2017, **158**, 1016–1025.

126 S. J. Oh, M. Burhan, K. C. Ng, Y. Kim and W. Chun, *Int. J. Energy Res.*, 2015, **39**, 965–976.

127 Y. Yu, M. Nakano and T. Ikeda, *Nature*, 2003, **425**, 145.

128 W. Feng, D. J. Broer and D. Liu, *Adv. Funct. Mater.*, 2020, **30**, 1901681.

129 Z. Zhang, C. Li, Y. Jia, Q. Gan, T. Ube, T. Ikeda, J. Wang and L. Jiang, *Adv. Mater. Technol.*, 2025, e01203.

130 J. Li, H. K. Bisoyi, J. Tian, J. Guo and Q. Li, *Adv. Mater.*, 2019, **31**, 1807751.

131 M. Camacho-Lopez, H. Finkelmann, P. Palffy-Muhoray and M. Shelley, *Nat. Mater.*, 2004, **3**, 307–310.

132 J. Yang, X. Zhang, X. Zhang, L. Wang, W. Feng and Q. Li, *Adv. Mater.*, 2021, **33**, 2004754.

133 P. Lv, X. Yang, H. K. Bisoyi, H. Zeng, X. Zhang, Y. Chen, P. Xue, S. Shi, A. Priimagi and L. Wang, *Mater. Horiz.*, 2021, **8**, 2475–2484.

134 X. Yang, Y. Chen, X. Zhang, P. Xue, P. Lv, Y. Yang, L. Wang and W. Feng, *Nano Today*, 2022, **43**, 101419.

135 Q. Liu, Z. C. Jiang, X. Jiang, J. Zhao, Y. Zhang, Y. Liu, J. B. Hou, Y. Y. Xiao, W. Pu and Y. Zhao, *Angew. Chem.*, 2025, **137**, e202500527.

136 X. Yang, L. Bai, X. Huang, G. Zhang, X. Lin, L. Li, Z. Zhang, G. Zhou, J. Lai and Y. You, *ACS Appl. Mater. Interfaces*, 2025, **17**, 51193–51200.

137 C. Zhu, S. Yang, M. Wang, Y. Zeng, L. Chu, W. Xie, P. Lan, L. Lan, G. Zhou and Z. Zhang, *J. Colloid Interface Sci.*, 2025, **695**, 137834.

138 M. Rogóż, J. Haberko and P. Wasylczyk, *Materials*, 2021, **14**, 6688.

139 T. Ube, H. Tsunoda, K. Kawasaki and T. Ikeda, *Adv. Opt. Mater.*, 2021, **9**, 2100053.

140 S. H. Choi, J. H. Kim, J. Ahn, T. Kim, Y. Jung, D. Won, J. Bang, K. R. Pyun, S. Jeong and H. Kim, *Nat. Mater.*, 2024, **23**, 834–843.

141 E. C. Davidson, A. Kotikian, S. Li, J. Aizenberg and J. A. Lewis, *Adv. Mater.*, 2020, **32**, 1905682.

142 D. Wu, Y. Zhang, H. Yang, A. Wei, Y. Zhang, A. Mensah, R. Yin, P. Lv, Q. Feng and Q. Wei, *Mater. Horiz.*, 2023, **10**, 2587–2598.

143 M. Yamada, M. Kondo, J.-i. Mamiya, Y. Yu, M. Kinoshita, C. Barrett and T. Ikeda, *Angew. Chem., Int. Ed.*, 2008, **47**, 4986–4988.

144 A. A. Elsayed, E. E. Khalil, M. A. Kassem and O. A. Huzzayin, *Renewable Energy*, 2021, **170**, 1129–1142.

145 K. Kumar, C. Knie, D. Bléger, M. A. Peletier, H. Friedrich, S. Hecht, D. J. Broer, M. G. Debije and A. P. H. J. Schenning, *Nat. Commun.*, 2016, **7**, 11975.

146 S. Liu, D. Zhang, F. Wang, S. Han, D. Yu and F. Li, *Opt. Express*, 2025, **33**, 7813–7829.

147 Y. Wang, A. Dang, Z. Zhang, R. Yin, Y. Gao, L. Feng and S. Yang, *Adv. Mater.*, 2020, **32**, 2004270.

148 M. Javed, T. Corazao, M. O. Saed, C. P. Ambulo, Y. Li, M. R. Kessler and T. H. Ware, *ACS Appl. Mater. Interfaces*, 2022, **14**(30), 35087–35096.

149 N. P. Skillin, G. E. Bauman, B. E. Kirkpatrick, J. M. McCracken, K. Park, R. A. Vaia, K. S. Anseth and T. J. White, *Adv. Mater.*, 2024, **36**, 2313745.

150 A. Athanassiou, M. Kalyva, K. Lakiotaki, S. Georgiou and C. Fotakis, *Adv. Mater.*, 2005, **17**, 988–992.

151 T. Hugel, N. B. Holland, A. Cattani, L. Moroder, M. Seitz and H. E. Gaub, *Science*, 2002, **296**, 1103–1106.

152 O. M. Tanchak and C. J. Barrett, *Macromolecules*, 2005, **38**(25), 10566–10570.

153 K. M. Lee, D. H. Wang, H. Koerner, R. A. Vaia, L.-S. Tan and T. J. White, *Angew. Chem., Int. Ed.*, 2012, **51**, 4117–4121.

154 S. V. Ahir and E. M. Terentjev, *Nat. Mater.*, 2005, **4**, 491–495.

155 N. Yan, Z. Zheng, Y. Liu, X. Jiang, J. Wu, M. Feng, L. Xu, Q. Guan and H. Li, *Nano Res.*, 2022, **15**(2), 1383–1392.

156 H. Zhang and Y. Zhao, *ACS Appl. Polym. Mater.*, 2024, **6**(16), 9685–9693.

157 J.-K. Sun, W. Li, C. Chen, C.-X. Ren, D.-M. Pan and J. Zhang, *Angew. Chem., Int. Ed.*, 2013, **52**, 6653–6657.

158 R. O. Al-Kaysi, A. M. Müller and C. J. Bardeen, *J. Am. Chem. Soc.*, 2006, **128**(50), 15938–15939.

159 T.-Y. Xu, F. Tong, H. Xu, M.-Q. Wang, H. Tian and D.-H. Qu, *J. Am. Chem. Soc.*, 2022, **14**, 6278–6290.

160 I. Tahir, E. Ahmed, D. P. Karothu, F. Fsehayem, J. M. Halabi and P. Naumov, *J. Am. Chem. Soc.*, 2024, **146**(44), 30174–30182.

161 H. Khandelwal, A. P. Schenning and M. G. Debije, *Adv. Energy Mater.*, 2017, **7**, 1602209.

162 Y. Ke, C. Zhou, Y. Zhou, S. Wang, S. H. Chan and Y. Long, *Adv. Funct. Mater.*, 2018, **28**, 1800113.

163 Y. Wang, E. L. Runnerstrom and D. J. Milliron, *Annu. Rev. Chem. Biomol. Eng.*, 2016, **7**, 283–304.

164 C. G. Granqvist, *Thin Solid Films*, 2014, **564**, 1–38.

3206 | *J. Mater. Chem. A*, 2026, **14**, 3185–3209

This journal is © The Royal Society of Chemistry 2026

165 A. J. Kragt, R. C. Loonen, D. J. Broer, M. G. Debije and A. P. Schenning, *J. Polym. Sci.*, 2021, **59**, 1278–1284.

166 C. Han, J. Lee, C. An and S. Oh, *Appl. Mater. Today*, 2023, **35**, 101923.

167 J. Yan, X. Fan, Y. Liu, K. Qu, Y. Yu and R.-Z. Li, *Appl. Mater. Today*, 2023, **32**, 101840.

168 Z.-Y. Kuang, Y. Deng, J. Hu, L. Tao, P. Wang, J. Chen and H.-L. Xie, *ACS Appl. Mater. Interfaces*, 2019, **11**, 37026–37034.

169 Y. Deng, S.-Q. Li, Q. Yang, Z.-W. Luo and H.-L. Xie, *Crystals*, 2021, **11**, 440.

170 W. Meng, Y. Gao, X. Hu, L. Tan, L. Li, G. Zhou, H. Yang, J. Wang and L. Jiang, *ACS Appl. Mater. Interfaces*, 2022, **14**, 28301–28309.

171 T. Wen, T. Ma, J. Qian, Z. Song, X. Jiang and Y. Yao, *Nat. Commun.*, 2024, **15**, 10821.

172 T. T. Larsen, A. Bjarklev, D. S. Hermann and J. Broeng, *Opt. Express*, 2003, **11**, 2589–2596.

173 P. Weis and S. Wu, *Macromol. Rapid Commun.*, 2018, **39**, 1700220.

174 A. P. Martinez, L. K. Decker, K. Wang, J. B. Kim, C. B. Murray and S. Yang, *Adv. Funct. Mater.*, 2025, **35**, 2422176.

175 W. Hou, J. Wang and J. a. Lv, *Adv. Mater.*, 2023, **35**, 2211800.

176 Y. He, L. Ren, Q. Liu, J. Xu, B. Wang, Z. Song, C. Xu, X. Zhou and B. Li, *Adv. Mater. Technol.*, 2025, **16**, e00078.

177 M. O. Saed, A. Gablier and E. M. Terentjev, *Chem. Rev.*, 2021, **122**, 4927–4945.

178 S. Yu, J. Chen, G. Gomard, H. Hölscher and U. Lemmer, *Adv. Opt. Mater.*, 2023, **11**, 2203134.

179 Y. Han, C. Jiang, H. Fu, C. Luo, H. Lin and H. Peng, *Energy Technol.*, 2020, **8**, 2000612.

180 S. Li, Y. Wang, Z. Liu, B. Chen, M. Liu, X. He and S. Yang, *Sci. Adv.*, 2025, **11**, eadt6136.

181 Y. Wang, A. Dang, Z. Zhang, R. Yin, Y. Gao, L. Feng and S. Yang, *Adv. Mater.*, 2020, **32**, 2004270.

182 Y. Xia, X. Zhang and S. Yang, *Angew. Chem.*, 2018, **130**, 5767–5770.

183 M. Zadan, D. K. Patel, A. P. Sabelhaus, J. Liao, A. Wertz, L. Yao and C. Majidi, *Adv. Mater.*, 2022, **34**, 2200857.

184 M. Wang, Z.-W. Cheng, B. Zuo, X.-M. Chen, S. Huang and H. Yang, *ACS Macro Lett.*, 2020, **9**, 860–865.

185 H. Tan, A. Jain, O. Voznyy, X. Lan, F. P. García de Arquer, J. Z. Fan, R. Quintero-Bermudez, M. Yuan, B. Zhang, Y. Zhao, F. Fan, P. Li, L. N. Quan, Y. Zhao, Z.-H. Lu, Z. Yang, S. Hoogland and E. H. Sargent, *Science*, 2017, **355**, 722–726.

186 H. Min, D. Y. Lee, J. Kim, G. Kim, K. S. Lee, J. Kim, M. J. Paik, Y. K. Kim, K. S. Kim and M. G. Kim, *Nature*, 2021, **598**, 444–450.

187 Y. Xue, X. Chen, F. Wang, J. Lin and J. Liu, *Adv. Mater.*, 2023, **35**, 2304095.

188 H. Choi, Y. Kim, S. Kim, H. Jung, S. Lee, K. Kim, H.-S. Han, J. Y. Kim, M. Shin and D. Son, *Nat. Electron.*, 2023, **6**, 779–789.

189 G. Chen, H. Feng, X. Zhou, F. Gao, K. Zhou, Y. Huang, B. Jin, T. Xie and Q. Zhao, *Nat. Commun.*, 2023, **14**, 6822.

190 A. Ryabchun, F. Lancia, J. Chen, R. Plamont, D. Morozov, B. L. Feringa and N. Katsonis, *Chem*, 2023, **9**, 3544–3554.

191 J.-a. Lv, Y. Liu, J. Wei, E. Chen, L. Qin and Y. Yu, *Nature*, 2016, **537**, 179–184.

192 L. T. de Haan, J. M. Verjans, D. J. Broer, C. W. Bastiaansen and A. P. Schenning, *J. Am. Chem. Soc.*, 2014, **136**, 10585–10588.

193 S. B. Lang, *Phys. Today*, 2005, **58**, 31–36.

194 G. Velarde, S. Pandya, L. Zhang, D. Garcia, E. Lupi, R. Gao, J. D. Wilbur, C. Dames and L. W. Martin, *ACS Appl. Mater. Interfaces*, 2019, **11**, 35146–35154.

195 Y. Wang, J. Sun, W. Liao and Z. Yang, *Adv. Mater.*, 2022, **34**, 2107840.

196 H. Lv, Y. Yao, M. Yuan, G. Chen, Y. Wang, L. Rao, S. Li, U. I. Kara, R. L. Dupont, C. Zhang, B. Chen, B. Liu, X. Zhou, R. Wu, S. Adera, R. Che, X. Zhang and X. Wang, *Nat. Commun.*, 2024, **15**, 1295.

197 H. Lv, Y. Yao, S. Li, G. Wu, B. Zhao, X. Zhou, R. L. Dupont, U. I. Kara, Y. Zhou, S. Xi, B. Liu, R. Che, J. Zhang, H. Xu, S. Adera, R. Wu and X. Wang, *Nat. Commun.*, 2023, **14**, 1982.

198 X. Zhang, J. Grajal, J. L. Vazquez-Roy, U. Radhakrishna, X. Wang, W. Chern, L. Zhou, Y. Lin, P.-C. Shen, X. Ji, X. Ling, A. Zubair, Y. Zhang, H. Wang, M. Dubey, J. Kong, M. Dresselhaus and T. Palacios, *Nature*, 2019, **566**, 368–372.

199 F. Gao, W. Li, X. Wang, X. Fang and M. Ma, *Nano Energy*, 2016, **22**, 19–26.

200 S. Uma and J. Philip, *J. Appl. Polym. Sci.*, 2014, **131**, 41142.

201 R. Whatmore, *Rep. Prog. Phys.*, 1986, **49**, 1335.

202 T. Zhao, W. Jiang, D. Niu, H. Liu, B. Chen, Y. Shi, L. Yin and B. Lu, *Appl. Energy*, 2017, **195**, 754–760.

203 H. Zhang, Y. Xie, X. Li, Z. Huang, S. Zhang, Y. Su, B. Wu, L. He, W. Yang and Y. Lin, *Energy*, 2016, **101**, 202–210.

204 Y. Yao, J. T. Waters, A. V. Shneidman, J. Cui, X. Wang, N. K. Mandsberg, S. Li, A. C. Balazs and J. Aizenberg, *Proc. Natl. Acad. Sci. U. S. A.*, 2018, **115**, 12950–12955.

205 Y. Wu, F. Wei, T. Li, M. Li, D. Pei and C. Li, *Chem. Eng. J.*, 2024, **489**, 151455.

206 Y. Zhang, J. Wang, X. Li, L. Chen and Q. Liu, *Chem. Eng. J.*, 2024, **503**, 158552.

207 H. Sun, W. Zhao, K. Ren, J. Guo and M. Zhou, *Chem. Eng. J.*, 2025, **511**, 162025.

208 S. T. Milner, T. D. Nguyen, M. D. Graham and N. L. Abbott, *Adv. Mater.*, 2021, **33**, 2103755.

209 A. S. Manzhos, L. J. Rupp and K. Nomura, *InfoMat*, 2023, **5**, e12113.

210 F. X. Gao, W. W. Li, X. Q. Wang, X. D. Fang and M. M. Ma, *Nano Energy*, 2016, **22**, 19–26.

211 S. Uma and J. R. Philip, *J. Appl. Polym. Sci.*, 2014, **131**, 41142.

212 R. W. Whatmore, *Rep. Prog. Phys.*, 1986, **49**, 1335–1386.

213 T. Zhao, W. Jiang, D. Niu, H. Liu, B. Chen and Y. Shi, *Appl. Energy*, 2017, **195**, 754–760.

214 H. Zhang, Y. Xie, X. Li, Z. Huang, S. Zhang, Y. Su, B. Wu, L. He and W. Yang, *Energy*, 2016, **102**, 368–376.

215 J. M. Hollerbach, I. W. Hunter and J. Ballantyne, *Rob. Rev.*, 1992, **2**, 307–308.

This journal is © The Royal Society of Chemistry 2026

J. Mater. Chem. A, 2026, **14**, 3185–3209 | **3207**

216 D. Črešnar, N. Derets, M. Trček, G. Skačej, A. Rešetič, M. Lavrič, V. Domenici, B. Zalar, S. Kralj and Z. Kutnjak, *J. Phys.: Energy*, 2023, **5**, 045004.

217 J. Shin, M. Kang, T. Tsai, C. Leal, P. V. Braun and D. G. Cahill, *ACS Macro Lett.*, 2016, **5**, 955–960.

218 J. Forman, O. Kilic Afsar, S. Nicita, R. H.-J. Lin, L. Yang, M. Hofmann, A. Kothakonda, Z. Gordon, C. Honnet and K. Dorsey, presented in part at the *Proceedings of the 36th Annual ACM Symposium on User Interface Software and Technology*, 2023.

219 J. Wang, Y. Wen, D. Pan, S. Lin, A. Chinnappan, Q. He, C. Liu, Z. Huang, S. Cai and S. Ramakrishna, *Nano Lett.*, 2024, **24**, 9990–9997.

220 S.-J. Ge, T.-P. Zhao, M. Wang, L.-L. Deng, B.-P. Lin, X.-Q. Zhang, Y. Sun, H. Yang and E.-Q. Chen, *Soft Matter*, 2017, **13**, 5463–5468.

221 H. Maeda, S. Wu, R. Marui, E. Yoshida, K. Hatakeyama-Sato, Y. Nabae, S. Nakagawa, M. Ryu, R. Ishige, Y. Noguchi, Y. Hayashi, M. Ishii, I. Kuwajima, F. Jiang, X. T. Vu, S. Ingebrandt, M. Tokita, J. Morikawa, R. Yoshida and T. Hayakawa, *npj Comput. Mater.*, 2025, **11**, 205.

222 S. Liu, C. Gao and Y. Xiong, *Adv. Funct. Mater.*, 2025, 2420723.

223 N. A. Zimbovskaya and A. Nitzan, *J. Chem. Phys.*, 2023, **158**, 234903.

224 Y. Wu, K. Wu, F. Xiao, W. Diao, D. He, H. Yang and J. Shi, *Macromol. Chem. Phys.*, 2023, **224**, 2300078.

225 N. Mehra, L. Mu and J. Zhu, *Compos. Sci. Technol.*, 2017, **148**, 97–105.

226 B. Sun and X. Huang, *npj Flexible Electron.*, 2021, **5**, 12.

227 J. Li, Y. Zhou, C. Jiang, D. Lei and X. Yu, *J. Mater. Chem. C*, 2024, **12**, 12179–12206.

228 C. L. Choy, *Polymers*, 1977, **18**, 984–1004.

229 Y. Cang, J. Liu, M. Ryu, B. Graczykowski, J. Morikawa, S. Yang and G. Fytas, *Nat. Commun.*, 2022, **13**, 5248.

230 J. B. St-Germain and Y. Zhao, *Chem. Commun.*, 2024, **60**, 11774–11777.

231 Q. Liu, Z. C. Jiang, X. Jiang, J. Zhao, Y. Zhang, Y. Liu, J. B. Hou, Y. Y. Xiao, W. Pu and Y. Zhao, *Angew. Chem.*, 2025, **137**, e202500527.

232 L. Xu, C. Zhu, S. C. Lamont, R. Tao, Y. Mao, Z. Guan, L. Zhang, J. Ding and F. J. Vernerey, *Adv. Funct. Mater.*, 2025, 2424033.

233 J. Sun, W. Liao and Z. Yang, *Adv. Mater.*, 2023, **35**, 2302706.

234 X. Tian, Y. Guo, J. Zhang, O. M. Ivasishin, J. Jia and J. Yan, *Small*, 2024, **20**, 2306952.

235 J.-H. Lee, S. Oh, I.-s. Jeong, Y. J. Lee, M. C. Kim, J. S. Park, K. Hyun, T. H. Ware and S.-k. Ahn, *Sci. Adv.*, 2025, **11**, eadt7613.

236 P. E. Silva, X. Lin, M. Vaara, M. Mohan, J. Vapaavuori and E. M. Terentjev, *Adv. Mater.*, 2023, **35**, 2210689.

237 Y. Liang, K. A. Treaster, A. Majumder, M. Settipalli, K. Panda, S. Godse, R. Roy, R. Mali, Z. Wang, Y. Luan, P. Hu, K. Searles, D. C. McLeod, K. A. Page, D. Bhagwandin, E. Meyhofer, P. Reddy, A. J. H. McGaughey, A. M. Evans and J. A. Malen, *ACS Nano*, 2025, **19**, 19009–19017.

238 M. Wang, J. Wang, H. Yang, B.-P. Lin, E.-Q. Chen, P. Keller, X.-Q. Zhang and Y. Sun, *Chem. Commun.*, 2016, **52**, 4313–4316.

239 Q. Wei, C. Uehara, M. Mukaida, K. Kirihara and T. Ishida, *AIP Adv.*, 2016, **6**, 045315.

240 W. Dai, L. Lv, T. Ma, X. Wang, J. Ying, Q. Yan, X. Tan, J. Gao, C. Xue and J. Yu, *Adv. Sci.*, 2021, **8**, 2003734.

241 N. Song, D. Jiao, S. Cui, X. Hou, P. Ding and L. Shi, *ACS Appl. Mater. Interfaces*, 2017, **9**, 2924–2932.

242 K. Wu, D. Liu, C. Lei, S. Xue and Q. Fu, *Chem. Eng. J.*, 2020, **394**, 124929.

243 A. Zandieh, P. Buahom, E. B. Shokouhi, L. H. Mark, R. Rahmati, O. A. Tafreshi, M. Hamidinejad, A. Mandelis, K. S. Kim and C. B. Park, *Nano Micro Small*, 2024, **20**, 2404189.

244 N. Zhao, J. Li, W. Wang, W. Gao and H. Bai, *ACS Nano*, 2022, **16**, 18958–18967.

245 Q. Chen, Z. Ma, Z. Wang, L. Liu, M. Zhu, W. Lei and P. Song, *Adv. Funct. Mater.*, 2021, **32**, 2110782.

246 X. He, K. Zhang, H. Wang, Y. Zhang, G. Xiao, H. Niu and Y. Yao, *Carbon*, 2022, **199**, 367–378.

247 X. Huang, P. Jiang and T. Tanaka, *IEEE Electr. Insul. Mag.*, 2011, **27**, 8–16.

248 X. Wang, F. L. Gao, H. Y. Zhao, L. Tian, S. Li, S. Wang, Z. Z. Yu and X. Li, *Adv. Funct. Mater.*, 2025, e12371.

249 M. Wu, Y. Xuan, X. Liu, Y. Jing and T. Li, *Adv. Funct. Mater.*, 2025, **42**, 2506229.

250 I.-L. Ngo, S. Jeon and C. Byon, *Int. J. Heat Mass Transfer*, 2016, **98**, 219–226.

251 S. J. Jeong and H. S. Lim, *Macromol. Res.*, 2025, 1–16.

252 D. J. Roach, C. Yuan, X. Kuang, V. C.-F. Li, P. Blake, M. L. Romero, I. Hammel, K. Yu and H. J. Qi, *ACS Appl. Mater. Interfaces*, 2019, **11**, 19514–19521.

253 F. Göktepe, Ö. Göktepe, R. H. Baughman, M. Zhang and J. Oh, *Adv. Mater. Technol.*, 2024, **9**, 2301971.

254 D. Štular, B. Tomšič, I. Jerman, B. Simončič, M. Mihelčič, L. Noč and I. G. Ilić, *Prog. Org. Coat.*, 2018, **124**, 213–223.

255 J. Tušek, K. Engelbrecht, R. Millán-Solsona, L. Mañosa, E. Vives, L. P. Mikkelsen and N. Pryds, *Adv. Energy Mater.*, 2015, **5**, 150361.

256 X. Moya and N. Mathur, *Science*, 2020, **370**, 797–803.

257 J. A. Herman, J. D. Hoang and T. J. White, *Small*, 2024, **20**, 2400786.

258 D. Cong, W. Xiong, A. Planes, Y. Ren, L. Mañosa, P. Cao, Z. Nie, X. Sun, Z. Yang and X. Hong, *Phys. Rev. Lett.*, 2019, **122**, 255703.

259 N. Candau, E. Vives, A. I. Fernández and M. L. Maspoch, *Polymer*, 2021, **236**, 124309.

260 M. Trček, M. Lavrič, G. Cordoyiannis, B. Zalar, B. Rožič, S. Kralj, V. Tzitzios, G. Nounesis and Z. Kutnjak, *Philos. Trans. R. Soc., A*, 2016, **374**, 20150301.

261 G. Skačej, *Liq. Cryst.*, 2018, **45**, 1964–1969.

262 T. Kim, W. Song, D.-Y. Son, L. K. Ono and Y. Qi, *J. Mater. Chem. A*, 2019, **7**, 2942–2964.

263 G. E. Blomgren, *J. Electrochem. Soc.*, 2016, **164**, A5019.

3208 | *J. Mater. Chem. A*, 2026, **14**, 3185–3209

This journal is © The Royal Society of Chemistry 2026

264 A. Manthiram, *J. Phys. Chem. Lett.*, 2011, **2**, 176–184.

265 S. Zhang and N. Pan, *Adv. Energy Mater.*, 2015, **5**, 1401401.

266 Y. Shao, M. F. El-Kady, J. Sun, Y. Li, Q. Zhang, M. Zhu, H. Wang, B. Dunn and R. B. Kaner, *Chem. Rev.*, 2018, **118**, 9233–9280.

267 T. Famprikis, P. Canepa, J. A. Dawson, M. S. Islam and C. Masquelier, *Nat. Mater.*, 2019, **18**, 1278–1291.

268 W. Zhao, J. Yi, P. He and H. Zhou, *Electrochem. Energy Rev.*, 2019, **2**, 574–605.

269 Q. Zhang, D. Soham, Z. Liang and J. Wan, *Med-X*, 2025, **3**, 3.

270 X. Ma, Z. Jiang and Y. Lin, *J. Semicond.*, 2021, **42**, 101602.

271 L. Wang, Y. Zhang and P. G. Bruce, *Natl. Sci. Rev.*, 2023, **10**, nwac062.

272 C. H. Rajapaksha, M. T. Gunathilaka, S. Narute, H. Albehaijan, C. Piedrahita, P. Paudel, C. Feng, B. Lüssem, T. Kyu and A. Jákli, *Molecules*, 2021, **26**, 4234.

273 L. Yang, Y. Liu, R. Bi, Y. Chen, C. Valenzuela, Y. Yang, H. Liu, L. Wang and W. Feng, *Adv. Funct. Mater.*, 2025, **39**, 2504979.

274 M. Wang, H. Zhang, Y. Li, R. Liu and H. Yang, *Chem. Eng. J.*, 2023, **476**, 146658.

275 Z. Zhu, R. Li and T. Pan, *Adv. Mater.*, 2018, **30**, 1705122.

276 M. G. Sumdani, M. R. Islam, A. N. A. Yahaya and S. I. Safie, *Polym. Eng. Sci.*, 2022, **62**, 269–303.

277 Y. Zhu, S. Murali, M. D. Stoller, K. J. Ganesh, W. Cai, P. J. Ferreira, A. Pirkle, R. M. Wallace, K. A. Cychosz and M. Thommes, *Science*, 2011, **332**, 1537–1541.

278 Z. Lu, J. Foroughi, C. Wang, H. Long and G. G. Wallace, *Adv. Energy Mater.*, 2018, **8**, 1702047.

279 M. Zhu, J. Wu, Y. Wang, M. Song, L. Long, S. H. Siyal, X. Yang and G. Sui, *J. Energy Chem.*, 2019, **37**, 126–142.

280 C. Ma, W. Cui, X. Liu, Y. Ding and Y. Wang, *InfoMat*, 2022, **4**, e12232.

281 M. Que, B. Zhang, J. Chen, X. Yin and S. Yun, *Mater. Adv.*, 2021, **2**, 5560–5579.

282 K. Xu, *Chem. Rev.*, 2004, **104**, 4303–4418.

283 D. T. Hallinan Jr and N. P. Balsara, *Annu. Rev. Mater. Res.*, 2013, **43**, 503–525.

284 Y. Zhao, C. Wu, G. Peng, X. Chen, X. Yao, Y. Bai, F. Wu, S. Chen and X. Xu, *J. Power Sources*, 2016, **301**, 47–53.

285 J. Qiu, X. Liu, R. Chen, Q. Li, Y. Wang, P. Chen, L. Gan, S. J. Lee, D. Nordlund, Y. Liu, X. Yu, X. Bai, H. Li and L. Chen, *Adv. Funct. Mater.*, 2020, **30**, 1909392.

286 A. M. Stephan, K. S. Nahm, M. A. Kulandainathan, G. Ravi and J. Wilson, *Eur. Polym. J.*, 2006, **42**, 1728–1734.

287 V. Aravindan, P. Vickraman and T. P. Kumar, *J. Non-Cryst. Solids*, 2008, **354**, 3451–3457.

288 H. Kim, J. Gibson, J. Maeng, M. O. Saed, K. Pimentel, R. T. Rihani, J. J. Pancrazio, S. V. Georgakopoulos and T. H. Ware, *ACS Appl. Mater. Interfaces*, 2019, **11**, 19506–19513.

289 L. Yang, Y. Liu, R. Bi, Y. Chen, C. Valenzuela, Y. Yang, H. Liu, L. Wang and W. Feng, *Adv. Funct. Mater.*, 2025, **39**, 2504979.

290 Z. Siddiquee, H. Lee, W. Xu, T. Kyu and A. Jákli, *Batteries*, 2025, **11**, 106.

291 R. Yan, X. Wang, S. Liu, Z. He, L. Wang and Z. Miao, *J. Alloys Compd.*, 2025, 183621.

292 K. Xie and B. Wei, *Adv. Mater.*, 2014, **26**, 3592–3617.

293 X. Gong, Q. Yang, C. Zhi and P. S. Lee, *Adv. Energy Mater.*, 2021, **11**, 2003308.

294 W. Liu, M. S. Song, B. Kong and Y. Cui, *Adv. Mater.*, 2017, **29**, 1603436.

295 R. K. Shaha, D. R. Merkel, M. P. Anderson, E. J. Devereaux, R. R. Patel, A. H. Torbati, N. Willett, C. M. Yakacki and C. P. Frick, *J. Mech. Behav. Biomed. Mater.*, 2020, **107**, 103757.

296 R. Shankar, T. K. Ghosh and R. J. Spontak, *Soft Matter*, 2007, **3**, 1116–1129.

297 R. E. Pelrine, R. D. Kornbluh and J. P. Joseph, *Sens. Actuators, A*, 1998, **64**, 77–85.

298 P. G. Madden, J. D. Madden, P. A. Anquetil, N. A. Vandesteeg and I. W. Hunter, *IEEE J. Oceanic Eng.*, 2004, **29**, 696–705.

299 T. Dayyoub, M. Zadorozhnyy, D. G. Ladokhin, E. Askerov, K. V. Filippova, L. D. Iudina, E. Iushina, D. V. Telyshev and A. Maksimkin, *J. Renewable Mater.*, 2025, **13**, 1267–1292.

300 V. De Luca, P. Digiamberardino, G. Di Pasquale, S. Graziani, A. Pollicino, E. Umana and M. G. Xibilia, *J. Polym. Sci., Part B: Polym. Phys.*, 2013, **51**, 699–734.

301 Z. S. Davidson, H. Shahsavan, A. Aghakhani, Y. Guo, L. Hines, Y. Xia, S. Yang and M. Sitti, *Sci. Adv.*, 2019, **5**, eaay0855.

302 Y.-Y. Xiao, Z.-C. Jiang, J.-B. Hou, X.-S. Chen and Y. Zhao, *Soft Matter*, 2022, **18**, 4850–4867.

303 T. Guin, H. E. Hinton, E. Burgeson, C. C. Bowland, L. T. Kearney, Y. Li, I. Ivanov, N. A. Nguyen and A. K. Naskar, *Adv. Intell. Syst.*, 2020, **2**, 2000022.

This journal is © The Royal Society of Chemistry 2026

J. Mater. Chem. A, 2026, **14**, 3185–3209 | **3209**